MODELING THE IMPACT OF CRACKING IN LOW PERMEABILITY LAYERS IN A GROUNDWATER CONTAMINATION SOURCE ZONE ON DISSOLVED CONTAMINANT FATE AND TRANSPORT

THESIS

Katherine W. Sievers, 2nd Lieutenant, USAF
AFIT/GES/ENV/12-M02

DEPARTMENT OF THE AIR FORCE
AIR UNIVERSITY
AIR FORCE INSTITUTE OF TECHNOLOGY

Wright-Patterson Air Force Base, Ohio

The views expressed in this thesis are those of the authors and do not reflect the official policy or position of the United States Air Force, Department of Defense or the United States Government.

AFIT/GES/ENV/12-M02

MODELING THE IMPACT OF CRACKING IN LOW PERMEABILITY LAYERS IN A GROUNDWATER CONTAMINATION SOURCE ZONE ON DISSOLVED CONTAMINANT FATE AND TRANSPORT

THESIS

Presented to the Faculty

Department of Systems and Engineering Management

Graduate School of Engineering and Management

Air Force Institute of Technology

Air University

Air Education and Training Command

In Partial Fulfillment of the Requirements for the

Degree of Master of Science in Environmental Engineering and Science

Katherine W. Sievers, BS

2nd Lieutenant, USAF

March 2011

APPROVED FOR PUBLIC RELEASE; DISTRIBUTION UNLIMITED

AFIT/GES/ENV/11-M02

MODELING THE IMPACT OF CRACKING IN LOW PERMEABILITY LAYERS IN A GROUNDWATER CONTAMINATION SOURCE ZONE ON DISSOLVED CONTAMINANT FATE AND TRANSPORT

Katherine W. Sievers, BS

2nd Lieutenant, USAF

Approved:

//signed//	14 Mar 2011
Mark N. Goltz, Ph.D. (Chairman)	Date
//signed//	14 Mar 2011
Avery H. Demond, Ph.D. (Member) University of Michigan	Date
//signed//	9 Mar 2011
Junqi Huang, Ph.D. (Member) U.S. Environmental Protection Agency	Date

Abstract

In this study, the subsurface storage and transport of a Dense Non-Aqueous Phase Liquid (DNAPL), trichloroethylene (TCE), was evaluated using a numerical model. DNAPLs are organic liquids comprised of slightly water-soluble chemicals or chemical mixtures that have a density greater than water. Many DNAPLs, such as TCE, are used as solvents by the DoD and industry. The improper disposal and handling of these chemicals has led to long term contamination of groundwater. In the subsurface, DNAPLs may pool atop low permeability layers, and even with the removal or destruction of most DNAPL mass, small amounts of remaining DNAPL which have been transported into the low permeability layer can dissolve into flowing groundwater and continue as a contamination source for decades. Recently developed models assume that transport in the low permeability zones is strictly diffusive; however field observations suggest that more mass is stored in the low permeability zones than can be explained by diffusion alone. This mass may be in the form of separate phase DNAPL or dissolved phase chlorinated aliphatic hydrocarbon (CAH). One explanation for these field observations is that there is enhanced transport of dissolved CAHs and/or DNAPL into the low permeability layers due to cracking. Cracks may allow for advective-dispersive flow of water contaminated with dissolved CAHs into the layer as well as possible movement of pure phase DNAPL into the layer. In this study, a numerical flow and transport model is employed using a dual domain construct (high and low permeability layers) to investigate the impact of cracking on DNAPL and CAH movement. Using literature values, crack geometry and spacing were varied to model and compare three

scenarios: (1) CAH diffusion into an uncracked low permeability clay layer; (2) CAH advection-dispersion into cracks, and (3) separate phase DNAPL movement into the cracks. For each scenario, model simulations are used to show the evolution and persistence of groundwater contamination down gradient of the DNAPL source caused by back diffusion of the contaminant out of the low permeability layer into flowing groundwater. This study found cracking will cause an increase in transport and storage of TCE in low permeability layers, resulting in down gradient concentrations above levels of concern for decades. Further, DNAPL phase TCE within cracks can significantly contribute to down gradient concentrations; however, the extent of this contribution is very dependent upon the rate of DNAPL dissolution. Given these findings, remediation goals may be difficult to meet if source remediation strategies are used which do not account for the effect of cracking upon contaminant transport and storage in low permeability layers.

Acknowledgements

I would like to acknowledge and thank my advisor, Dr. Mark Goltz for providing me the opportunity to work together on this research. The discussions, timely edits, and encouragement were greatly appreciated and immensely helpful in completion of this thesis. Dr. Junqi Huang at the Robert S. Kerr Environmental Research Center (USEPA) was also immensely helpful in determining the proper research methods and application of the models used in this thesis. His quick and thorough responses enabled us to identify and solve problems in the model quickly. I would also like to thank Dr. Avery Demond at the University of Michigan for her guidance, and her students Margarita Otero and Derya Ayral for in depth explanations of cracking and experimental results. I would also like to thank the Strategic Environmental Research and Development Program (SERDP) for the funding making this research possible. Finally, I would like to thank my husband for all of his love and support throughout this process.

Katherine W. Sievers

Table of Contents

Page Number

List of Figures

List of Tables

MODELING THE IMPACT OF CRACKING IN LOW PERMEABILITY LAYERS IN A GROUNDWATER CONTAMINATION SOURCE ZONE ON DISSOLVED CONTAMINANT FATE AND TRANSPORT

1. Introduction

1.1 Background

Widespread use of chlorinated solvents such as tetrachloroethene (PCE) and trichloroethene (TCE) in industrial operations over the last century has resulted in extensive groundwater contamination. Poor handling and disposal of these chlorinated solvents has led to a multitude of contaminated sites throughout both the DoD and industry. The EPA estimates that over 60% of Superfund sites are contaminated with chlorinated solvents. If these sites are in close proximity to a water supply, those who ingest the water are at an increased risk for developing liver problems and cancer (EPA, 2011). The solubility of many chlorinated solvents may be as high as several g/L, which exceeds the drinking water standard by a factor of 10^6 (EPA, 2011). The Environmental Protection Agency has established a maximum contaminant level (MCL) for TCE in drinking water, the contaminant that is the focus of this study, of 5 parts per billion, or 5μg/L.

When chlorinated solvents are spilled or leaked onto the ground, they move downward as a dense separate phase immiscible liquid or "DNAPL" (dense nonaqueous phase liquid). Since DNAPLs have a specific gravity greater than water, when they reach the water table, they continue their downward migration until they encounter low permeability layers. The DNAPL will form pools atop these layers. These pools serve as

a persistent contaminant source as the chlorinated compound dissolves into the flowing groundwater. In this study, we will refer to dissolved phase chlorinated compound as a "CAH" (chlorinated aliphatic hydrocarbon). Also, as the DNAPL migrates downward, small amounts of residual DNAPL are left behind in the pore spaces between the aquifer solids. This residual DNAPL serves as another source of persistent contamination as it dissolves into groundwater. The flowing groundwater which transports the CAH will form a plume. Plumes vary in length depending upon the total mass of the contaminant, contaminant properties and aquifer conditions. Water will flow quickly through the high permeability layers and slowly through the low permeability layers. Figure 1 is a conceptual model showing DNAPL distribution in the subsurface, as well as the plume that forms as groundwater flows past the DNAPL pools and residual.

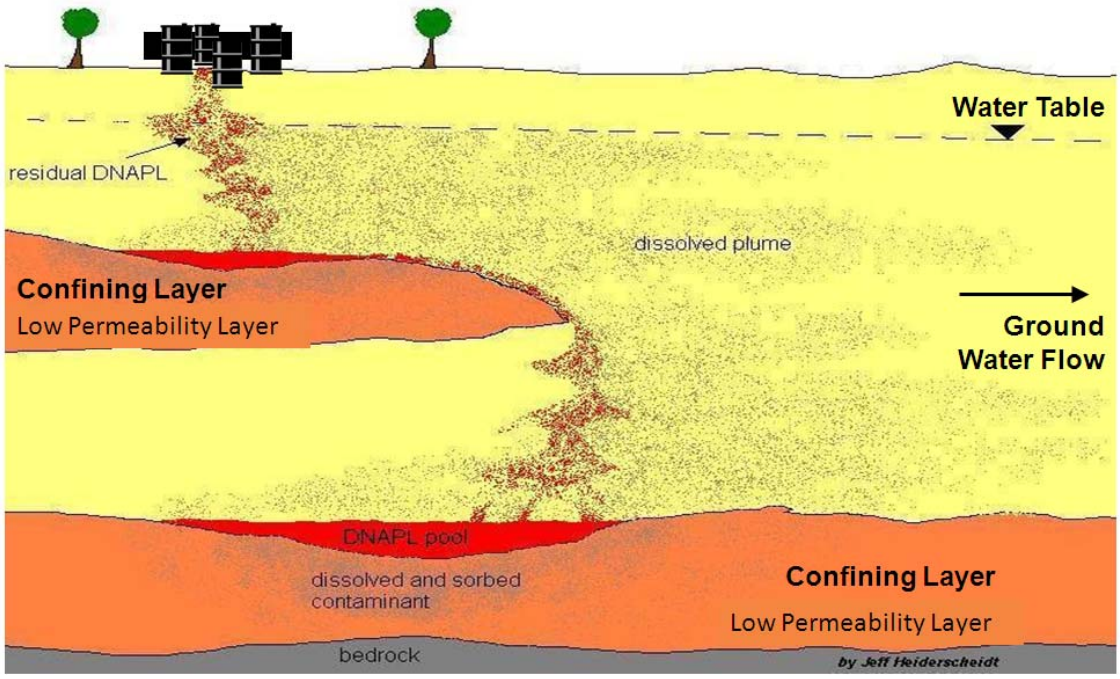

Figure 1-A: DNAPL Distribution in the Subsurface (after Heiderschiedt, 2010)

The DNAPL will tend to migrate down through the high permeability layers, pool atop the low permeability layers, and slowly enter the low permeability layers either as a CAH or DNAPL. During source zone remediation, various technologies may be used to remove or destroy the DNAPL pools and residual. However, even if all the separate phase residual and pooled DNAPL is removed from the high permeability zones, if enough contaminant is stored within the low permeability layer it can continue to act as a long-term contaminant source. The contaminant can be stored in the low permeability layer in the dissolved phase or the DNAPL phase. These long-term sources can continue to contaminate drinking water as well as extend the cost and timeline to achieve remediation.

As described above, DNAPL and/or dissolved chlorinated compound stored in low permeability lenses and layers in the subsurface can create a persistent source of contamination. The cleanup of low permeability lenses is very difficult and often long-term contamination continues to exist at sites after the remediation is considered complete (AFCEE, 2007). The movement into these low permeability layers is typically modeled as Fickian diffusion, with the diffusion coefficient modified to account for the tortuosity of the low permeability material, as well as for retardation due to contaminant sorption to the solids making up the layer (Parker et al., 2008). Recently, however, the applicability of this Fickian model has been questioned, and the potential for enhanced transport in these low permeability layers is being studied (Miniter, 2011).

One hypothesis for the enhanced transport is that the low permeability materials contain cracks. Cracks naturally occur in clay layers and can be caused by releases of

pressure due to erosion, excavation, or changes in water table levels (McKay et al., 1993). Cracking is dependent upon site formation, lithology, and composition. Another hypothesis is that the interaction of the DNAPL mixture with low permeability lenses in the contamination source areas can result in an alteration of the properties and physical structure of the low permeability lenses (Demond, 2010). This alteration may also lead to cracking. Thus, cracking of low permeability materials, whether due to natural processes or the interaction of a DNAPL mixture with the low permeability lenses, may result in enhanced transport of contaminant into (and out of) the lenses. This enhanced transport may result in: (1) advective transport of dissolved solvent, (2) DNAPL entry into the cracks, and/or (3) enhanced diffusion of dissolved solvent into the cracks, as the cracks have lower tortuosity than the surrounding matrix.

It has been reported when a NAPL is in contact with low permeability clay layers that the hydraulic conductivity of the layers can increase by one to five orders of magnitude. This increase in hydraulic conductivity has been ascribed to interlayer compression (Brown and Thomas, 1987). The shrinking of the clay layers leads to the formation of cracks and micro fractures and a concomitant increase in hydraulic conductivity. If either dissolved or pure phase DNAPL enters these cracks, diffusion into the low permeability matrix will greatly increase due to a larger contact area. Both naturally occurring cracks and cracks that are the result of DNAPL interaction can be classified by aperture size, depth, surface geometry, surface markings, fabric classification, and spacing (Denness and Fookes, 1969). This work will only include the effects of crack aperture, depth, and spacing.

In order to quantify the impact of cracking on contaminant transport, a dual-domain model was developed. The model represented cracks as a so-called "mobile domain", with transport of dissolved DNAPL controlled by advection, dispersion, and diffusion. The clay matrix was represented as an immobile domain, where diffusion and equilibrium sorption controlled transport (Miniter, 2011). A first-order rate constant described dissolved DNAPL transport between the two domains. A model scenario was constructed where a pool of DNAPL sat within a high permeability sand layer atop cracked clay for a period of time. The model was used to simulate concentrations as a function of time down gradient of the DNAPL source. It was shown that the existence of cracks in the clay led to increased concentrations of dissolved DNAPL downgradient, well after the source had been removed (Miniter, 2011).

1.2 Research Objective

The primary objective of the research is to model the impact of cracks, either naturally occurring or due to the interaction between DNAPLs and low permeability lenses in contamination source zones, focusing on the storage and transport of chlorinated solvents within these lenses, and the subsequent impact on downgradient dissolved contaminant concentrations. A model that simulates enhanced diffusion into low permeability lenses that was previously developed by Miniter (2011) will be further developed to model: (1) diffusion only into the cracks and surrounding matrix, and (2) separate phase DNAPL transport into the cracks. Results from these simulations will be compared with earlier conceptualizations that assume: (1) diffusion into uncracked clay (AFCEE, 2007), and (2) advective/dispersive transport in cracks and diffusion in clay

(Miniter, 2011). Properties of the cracks and matrix will be found in the literature and incorporated in the model. The model will be applied to simulate changes in dissolved plume behavior resulting from cracks, that may either be naturally occurring or DNAPL induced, in low permeability clay.

1.3 Research Questions

1. What are the typical characteristics of existing cracks in low permeability layers?
2. What is the effect of cracking on the transport of contaminants into and out of low permeability layers?
3. What mathematical models can be used to simulate transport (e.g. advection, dispersion, diffusion, and DNAPL transport) into and out of cracks in low permeability layers?
4. Compared to an uncracked source zone, how is the flow different at a cracked source zone?
5. What is the effect of enhanced transport into low permeability layers on dissolved plume longevity and evolution?

1.4 Research Methodology

1. The initial phase of the study involved a literature review to a) determine if significant cracking occurs naturally in low permeability layers, b) obtain parameters to characterize these naturally occurring cracks, and c) determine the appropriate model to integrate these parameters into flow and transport equations.

2. Expand the existing Miniter (2011) model to include diffusion and pure phase DNAPL movement into cracks as mass transport processes.
3. Use the Miniter (2011) and AFCEE (2007) models, as well as the extended models developed in the previous step, to quantify and compare the effects of cracking. The comparison will consider the following transport processes: (1) diffusion only into cracks, (2) advection-dispersion into cracks, (3) pure phase DNAPL movement into the cracks, and (4) diffusion into uncracked clay.

1.5 Scope and Limitations of Research

The modeling done in this research examines highly idealized systems to examine the possible impact of cracking in subsurface systems. This research should not be used to predict specific concentrations, rather it provides a qualitative understanding of DNAPL plume behavior. The values used for simulations are based on common values and trends found in literature, not a specific site. The model used in this study assumes (1) no degradation or sorption of the contaminant, (2) the subsurface material properties in each layer are homogeneous with respect to space and time, (3) steady state flow, and (4) that cracks can be effectively simulated with slight changes to properties in a homogeneous medium. These assumptions are necessary for both model execution and to create comparisons between different scenarios. The breakthrough curves and mass balance analyses presented are presumed to be an accurate comparison of the effects on down gradient plume concentration under different cracking scenarios.

1.6 Definitions

Advection – Flow as the result of an externally applied pressure difference or as a result of gravity/density changes

Basal Spacing - Spacing between adjacent layers of a crystalline structure

Chlorinated Aliphatic Hydrocarbon (CAH) – The term used for the dissolved phase DNAPL

Crack – An opening in a material caused by an applied stress that allows fluid to freely enter the material

Dense Non Aqueous Phase Liquid (DNAPL) – A fluid which has a density greater than water and is also relatively immiscible in water

Diffusion – Movement of a dissolved solute governed by a concentration gradient according to Fick's Law

Dispersion – Spreading of mass due to spatial and temporal variations of velocity in a flow field. In this work dispersion is modeled as a Fickian process to capture the heterogeneity of actual porous media

Dissolution – The process of dissolving (e.g., from a DNAPL phase to a dissolved phase)

Enhanced Diffusion – The increased amount of diffusion into porous medium than can be predicted by models conventional diffusion models governed by Fick's Law

Entry Pressure – The pressure required for a DNAPL to enter a crack

Hydraulic Conductivity – The capacity of a medium to transmit water

Maximum Contaminant Level (MCL) – Legal limit for a contaminant in drinking water set forth by the Environmental Protection Agency

Permeability – The ease with which fluid can move through porous material

Retardation – Process by which the velocity of the contaminant becomes less than the velocity of the water due to sorption

Sorption – The binding of a contaminant to a porous medium

1.7 Definition of Units

In this work, when defining variables in equations the units will follow the variable in brackets. A list of units is shown below.

F – Force

L – Length

M – Mass

T – Time

2. Literature Review

2.1 Overview

Understanding the processes which govern contaminant transport in aquifers is vitally important in setting and achieving remediation goals. The goal of this research is to achieve a deeper understanding of why concentrations down gradient of sources may remain in excess of MCLs for decades. Due to gravity, a DNAPL will move downward through the saturated zone of porous media until the DNAPL encounters low permeability layers where it spreads, forming pools. The pools of DNAPL will slowly dissolve into flowing groundwater, as well as diffuse into the low permeability matrix. These sources create dilute plumes which can extend for miles. The diffusion into the low permeability matrix also means contaminants will diffuse back into the flowing groundwater, perpetuating the plume, even after the pool has been removed or completely dissolved. This chapter examines mechanisms by which the contaminant is transported into the low permeability matrix. The contaminant may enter the matrix through three possible routes: (1) diffusion of the CAH into the uncracked matrix, (2) advection, dispersion, and diffusion of the CAH into the cracked matrix, and finally, (3) advection of the DNAPL into cracks combined with diffusion of the CAH into the surrounding matrix.

2.2 Aquifer Characteristics

An aquifer is commonly accepted to be a very heterogeneous medium. Aquifers can be made out of cracked rock, cobbles, gravel, sand, clay, silt, or most commonly a combination of many different materials. Water will flow through an aquifer based on

pressure gradients and hydraulic conductivity. The water flows through the medium in accordance with Darcy's Law, moving from areas of high hydraulic head to areas of low head. This means water can flow horizontally, transversely, and vertically. This thesis considers flow through sand and clay only. Based on the relative hydraulic conductivities of sand and clay, water will flow quickly through sand and extremely slowly through clay. Sand is considered a high permeability medium while clay is considered a very low permeability medium.

2.2.1 Naturally Occurring Cracking

Cracking occurs naturally in low permeability layers, and these cracks may allow for enhanced flow and transport of contaminants. The hydraulic conductivity of cracked clay is commonly two to three times higher than uncracked clay (McKay et al., 1993). Cracks can be formed at extensive depths from weathering or stress relief, explaining their occurrence in most glacial till (Mackay et al., 2000).

Important crack characteristics include aperture, spacing, and depth. Crack apertures generally cannot be measured directly, therefore many investigators approximate crack apertures in field and laboratory studies using the cubic law. The cubic law uses hydraulic data, and an important assumption is that the crack walls are two smooth parallel plates, to estimate crack aperture (Sims et al., 1996). The cubic law is shown below in Equation 2.1:

$$Q_F = (2b)^3 \frac{\rho g}{12\mu} W \frac{\Delta H}{\Delta L} \qquad \text{Equation 2.1}$$

Q_F [L^3T^{-1}] is the flow rate through the crack, ρ [ML^{-3}] is the fluid density, g is gravitational acceleration [LT^{-2}], μ [$ML^{-1}T^{-1}$] is the dynamic viscosity of the fluid, 2b [L]

is the aperture width, W [L] is width of the sample, ΔH [L] is the head drop over the length of the crack, and ΔL [L] is the crack length (Sims et al., 1996).

McKay et al. (1993) conducted an extensive field scale investigation in order to reliably estimate the magnitude and distribution of crack characteristics in a clay deposit. Previously calculated aperture estimates were based on an average of hydraulic conductivity measurements for a small number of measurements. McKay et al. (1993) selected the Laidlaw site in Lambton County, Ontario due to the extensive knowledge base established by previous studies. The cubic law was used to determine crack aperture. Transport of aqueous contaminants at the Laidlaw site was expected to be governed by: (1) advection through the cracks, (2) diffusion into the matrix pore water, and (3) retardation and degradation processes (sorption, precipitation, biodegradation) in the cracks and surrounding matrix (McKay et al., 1993). All of these processes are highly dependent upon cracks. Interestingly, 90% of the cracks in the upper 3.5m had apertures less than 21 μm, although apertures did range from 1 to 43 μm (McKay et al., 1993). The aperture results from the Laidlaw site were similar to other sites, suggesting these values are typical for glacial till.

A study conducted by O'Hara et al. (2000) estimated the size and variability of crack apertures. The methods used were (1) conventional hydraulic tests, (2) immiscible-phase fluid entry, (3) and channel identification using diffusion halos along cracks. The laboratory study used a column which was 0.5 m in diameter and 0.5 m in length. The column was extracted from between 3.7 and 4.2 m depth in a surficial, slightly weathered, clay deposit. Flowing water and DNAPL phase TCE were used to identify areas of channeled flow in the cracks. Although horizontal cracks did exist, below 2 m

nearly all cracks were found to be vertical (O'Hara et al., 2000). The mean hydraulic conductivity in the cracked clay was found to be three times greater than in the uncracked clay, and the average aperture range was found to be between 8 and 11 μm (O'Hara et al., 2000). The study found that a low average hydraulic conductivity does not necessarily mean low contaminant transport in cracked clay.

Sims et al. (1996) studied samples from a weathered cracked clay till deposit using a flexible permeameter. The samples used were from the Laidlaw Environmental Services hazardous waste disposal site located near Sarnia, Ontario. The cracks at the site are generally attributed to desiccation (Sims et al., 1996). The clay samples were gathered between 4 and 5 meters below land surface. Sample locations were identified by the crack halos shown in Figure 2.1.

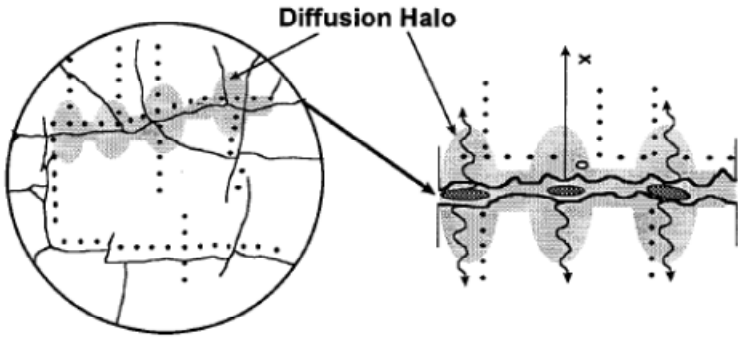

Figure 2-A: Diffusion halos surrounding cracks (Sims et al., 1996)

The crack halos appeared stained due to oxidation of matrix material. The highly oxidized halos are indicative of recently flowing groundwater (Sims et al., 1996). Two colors of halos were observed at the site, black/brown and grey/green. The black/brown coloration of the halos was determined to indicate active flowing oxygenated ground

water, which resulted in staining due to manganese and iron oxidation. The grey/green halos indicated a lesser amount of oxygenated groundwater flow. It was determined the grey/green halos were associated with dead end cracks, meaning offshoots from larger cracks that would not allow significant amounts of groundwater movement. The grey/green halos and associated cracks were most abundant at a depth of 4 meters and were selected for study (Sims et al., 1996).

Samples were gathered by using a 70mm Shelby tube over isolated halos. The tube was driven 40 cm into the till. The sample was sheared from the surrounding clay to minimize causing an increase in cracks. The samples were stored at 4˚C and sealed in beeswax to prevent further desiccation. Flow tests were conducted and crack apertures were back calculated using Equation 2.1, the cubic law relationship. The crack apertures were found to range between 0 and 5 μm. McKay et al. (1993) found crack apertures to range between 1 and 43μm at the same site, and Sims et al. (1996) suggested that the discrepancies between their lab based findings and those obtained in the field were because samples gathered for lab testing were not representative of field conditions due to: (1) the larger apertures observed in the field may have become plugged or filled when extracted and transported to the lab, (2) the small cracks used in the lab do not represent field scale processes such as flow channeling, and (3) cracks which were open in the field may have closed during sampling or lab preparation.

A summary of crack apertures, depths, and spacing from various studies is shown below in Table 2.1. The depth listed is the deepest measurement point and does not necessarily indicate the depth at which the crack ends.

Table 2-1: Crack characteristics found in the literature

Reference	Depth (m)	Spacing (m)	Aperture (μm)
D'Astous et al. (1989)	<4	0.04-0.1	26-32
Day (1977)	<18	0.05-0.15	1-14
Grisak (1980)	<7	0.04	4
Henry et al. (1986)	<16	0.4	50
Hinsby et al. (1996)	2-2.5	-	1-120
Keller et al. (1986)	12-18	<.15	11
McKay et al. (1993) (2)	1.7-3.2	0.04-0.13	9-43
McKay et al. (1993)	<5	0.02-1.0	<43
Pankow et al. (1984, 1986)	<4	0.03	150
O'Hara et al. (2000)	3.7-4.2	-	5-17
Rudolph et al. (1991)	<20	1.5	30
Sims et al. (1996)	4-5	-	1-5
Thompson (1990)	40-50	1.2-5	140-210

2.2.2 DNAPL Caused Cracking

While cracks occur naturally in nature, pooled DNAPL also can alter the physical properties of clay. Many studies have examined the impact of organic liquids on basal spacing. Basal spacing is the spacing between adjacent layers of a crystalline structure, in general as basal spacing increases hydraulic conductivity decreases. Clay minerals are considered crystalline structures. A clayey deposit will generally contain a significant amount of clay minerals, for example the clay mineral content at the aquitard in Dover AFB, DE ranged between 18 and 35% (Ball et al., 1997).

Many studies have examined the impact of organic solvents on basal spacing. One study by Brown and Thomas (1987) studied the mechanism by which an organic liquid can change the hydraulic conductivity of a clay by measuring basal spacing, electrophoretic mobility, zeta potential, flocculation, and volume change. The clays used were illite, smectite, and kaolinite. The organic liquids used in this study were acetone and ethanol. Brown and Thomas (1987) found that the hydraulic conductivity was significantly greater in kaolinitic mixtures exposed to acetone. Further, solutions that were 70% or more acetone caused the same effects as pure acetone. The illitic mixtures exhibited small increases in hydraulic conductivity. Dilute acetone solutions (2-5%) caused significant increases in basal spacing, which should lead to a decreased hydraulic conductivity. Brown and Thomas (1987) also found that all clays when in contact with an organic solution would swell to varying degrees. Brown and Thomas (1987) concluded that as organic liquids displace water in equilibrium with clay soil, the soil will shrink, causing cracks to form. These cracks can act as channels for liquids to flow. This results in an increase in hydraulic conductivity.

Ayral et al. (2011) found evidence that a spilled DNAPL can cause cracking in an otherwise unfractured aquitard. Three hypotheses are proposed by the researchers for the formation of cracks, (1) organics liquids decrease the basal spacing compared to water, "desiccating" the clay (2) surfactants in the waste can change the wettability (water wet to organic wet), enhancing the transport of the organic liquid, and (3) interparticle changes (floculation) (Personal Communication, 2012). Only the first hypothesis is discussed in this literature review. Ayral et al. (2011) compared the effects of various organics on

basal spacing including the pure organic liquid solvent TCE with a waste sample of TCE. Waste DNAPLs are typically mixtures and will include other compounds such as surfactants. The changes in basal spacing of montmorillonite in contact with various organics were examined in this study. Tests showed the basal spacing was smaller when saturated with pure TCE and waste TCE in comparison to when saturated with water (Ayral et al., 2011). The basal spacing of montmorillonite was examined when saturated with a surfactant. While the basal spacing increased as compared to water, the basal spacing of the waste TCE remained closer to the basal spacing of pure TCE. This suggests the spacing is dominated by the solvent matrix as opposed to the presence of surfactants. Interestingly, Aryal et al. (2011) found that trichlorinated organic solvents cause a smaller increase in basal spacing than monochlorinated or dichlorinated organics.

In the laboratory, clays were left in contact with TCE waste for an extended period of time. Figure 2.2 (a) depicts a crack forming after being exposed to TCE waste for ten days, and Figure 2.2 (b) depicts increased cracking after being exposed to TCE waste for fifty days. Figure 2.3 displays the vertical growth of cracks (Personal Communication, 2012).

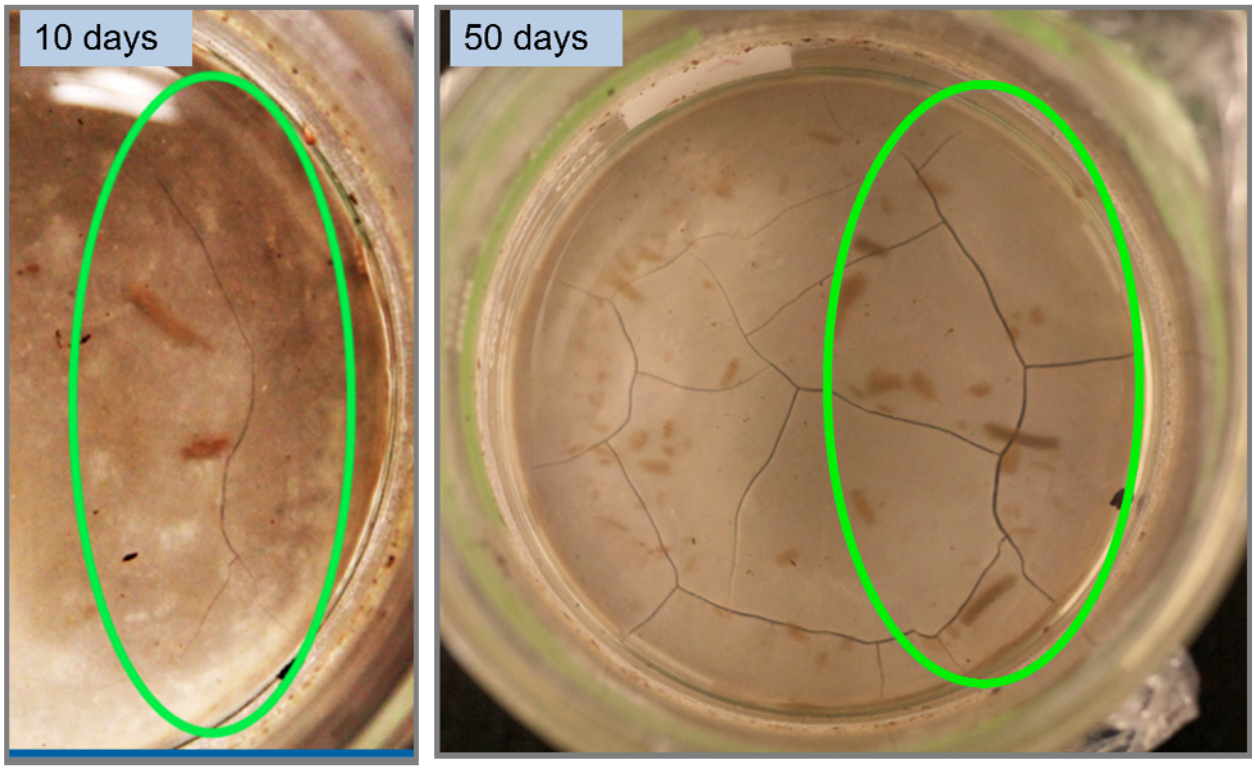

Figure 2-B: (a) Crack formation at 10 days, (b) crack formation at 50 days

Figure 2-C: Vertical Crack Formation

2.3 Diffusion of the CAH

2.3.1 Conceptual Model

Transport of CAHs into low permeability layers is assumed to be governed by simple Fickian diffusion, meaning CAH molecules will move preferentially from zones of high concentration to low concentration due to Brownian motion. Mass transfer into the low permeability layers will occur due to the relatively high concentrations of CAH found around the DNAPL pool and residuals. The net result of the relative immobility of the pore water in the low permeability matrix is long-term contaminant accumulation and high contaminant mass storage.

Back diffusion has been hypothesized to cause long-term plume persistence. The term back diffusion refers to diffusion of contaminants out of low permeability layers into adjacent high permeability zones. Due to lower concentration gradients driving back diffusion, back diffusion is thought to be a much slower process than the initial diffusion process (Sale et al., 2008). Although back diffusion is slow, it can contribute enough mass to the flowing groundwater to propagate plumes in excess of MCLs for decades.

Parker et al. (2008) concluded that back diffusion from one or a small number of thin clayey layers in a sand aquifer can cause down gradient concentrations to remain above MCLs for many years after source containment or removal. A site heavily contaminated with TCE in Florida was studied after a site remediation failed to achieve results predicted by calculations. Parker et al. (2008) compared three hypotheses for the cause of plume persistence after the source zone had been removed. These three hypotheses were: (1) incomplete source zone removal, (2) DNAPL occurrence down

gradient, and, (3) back diffusion from one or more thin clay layers. In their study, Parker et al. (2008) eliminated the first two hypotheses, leaving back diffusion as the only plausible hypothesis. The study found that even a clay layer of less than 0.2 m thickness can cause "plume persistence due to back diffusion for several years or even decades after the flux from the source is completely isolated" (Parker et al., 2008). The concentrations observed in the plumes from CAH stored in these thin clay layers were found to exceed the published MCLs.

2.3.2 Analytical Model

To investigate the movement of solutes into clay, Johnson et al. (1989) examined cores of uncracked clay near a site studied by Goodall and Quigley (1977) and Crooks and Quigley (1984). These cores were exposed to contaminants and were then analyzed for chlorides, organics, and total organic carbon. Concentration profiles for each core were developed, and the distribution of chloride was examined to analyze impacts of diffusion. Chloride concentrations in each core were high at the surface where the clay was in contact with the waste and decreased as clay depth increased. These profiles suggested the primary mechanism of transport was diffusion and the profiles were modeled using Equation 2.2, Fick's second law,

$$\frac{\partial C}{\partial t} = D_{eff}\frac{\partial^2 C}{\partial z^2} \qquad \text{Equation 2.2}$$

where C [ML^{-3}] is concentration, t is time, D_{eff} [L^2T^{-1}] is the effective solute diffusion coefficient, and z is the vertical direction. D_{eff} is given by Equation 2.3:

$$D_{eff} = D_0\tau \qquad \text{Equation 2.3}$$

The free solution diffusion coefficient (D_0) cannot be accurately used in diffusion equations due to the tortuous path particles follow in porous media. The tortuosity (τ) ranges between 0 and 1 and accounts for the complex and indirect flowpath solutes travel through a porous medium. While the chloride reached maximum depths of 83 cm, organic solutes were not detected past a depth of 15 cm. Johnson et al. (1989) concluded the differences in diffusion between the chloride and organic solutes was due to the sorption of the organics to clay. The effect of sorption is related to both soil and chemical properties. Commonly the effects of sorption to the immobile clay phase can be represented by a retardation factor (R_{imm}) [-] given by Equation 2.4,

$$R_{imm} = 1 + \frac{\rho_b K_d}{\theta} \qquad \text{Equation 2.4}$$

where ρ_b [M^1L^{-3}] is the clay bulk density, θ [-] is the porosity of clay, and K_d [$M^{-1}L^3$] is the sorption partition coefficient. R_{imm} is incorporated into Equation 2.4 to give Equation 2.5 and 2.6.

$$D_{eff} = \frac{D_0 \tau}{R_{imm}} \qquad \text{Equation 2.5}$$

$$\frac{\partial C}{\partial t} = \frac{D_0 \tau}{R_{imm}} \frac{\partial^2 C}{\partial y^2} \qquad \text{Equation 2.6}$$

The model employed by Johnson et al. (1989), which used Equation 2.6, produced results consistent with observed concentrations in uncracked clay.

Removing the remaining DNAPL from the source at a contaminated site is commonly the first step in site remediation. The goal of source cleanup is to remove the source of the dissolved contaminant plume. Sale et al. (2008) investigated how source removal will affect down gradient plume concentrations. Laboratory and analytical modeling experiments were conducted with a source that had a DNAPL accumulate

above a low permeability capillary barrier (Sale et al., 2008). A laboratory study was conducted using two common DNAPLs: PCE and TCE, and a light non-aqueous phase liquid (LNAPL), methyl-tert-butyl-ether (MTBE). The chemicals were introduced into highly idealized laboratory experimental boxes with a high permeability transmissive zone above a low permeability clay zone. The assumed mechanism of transport was diffusion only. The sources were introduced and then removed after 25 days. Mass transport was then evaluated for another 58 days. The study found that 15-44% of the contaminant mass was stored in the low permeability clay layer (Sale et al., 2008). The analytical model, which predicted results found in the laboratory, then was applied to simulate longer periods of time allowing for diffusion out of the low permeability clay layer. In the analytical modeling, the source was present for the first 1000 days and then removed. Down gradient concentrations remained high for over 20 years, with the concentration in the media 1m from the source decreasing much more rapidly than the concentration 100m from the source (Sale et al., 2008). This suggests the plume itself can act as a secondary source of contamination, causing contamination of clay down gradient of the DNAPL source due to diffusion from the dissolved plume into the clay.

2.3.3 Numerical Model

Parker et al (2004) modeled TCE transport in an unfractured minimally weathered silt aquitard. At the site, TCE DNAPL accumulated at the bottom of a 10m thick sand aquifer atop a 20m thick silt aquitard. An understanding of TCE transport through the aquitard ws needed due to the pumping of drinking water in an underlying sand aquifer. A one dimensional numerical diffusive transport model was applied to the site to

determine the maximum depth to which the aqueous TCE fronts reached. The hydraulic as well as diffusive properties were determined using a one year in situ tracer study. The model was verified examining cores at the site that had been exposed for 35-45 years. The cores verified the uncracked, unweathered nature of the aquitard and indicated that transport was diffusion-dominated. Two scenarios were considered: a time period of 1200 years with no advection through the aquitard and a time period of 500 years with a strong vertical hydraulic gradient through the silt aquitard. The model predicted the TCE would reach the underlying aquifer, however the concentrations reaching pumping wells would not be above MCLs (Parker et al., 2004).

Chapman and Parker (2011) investigated the ability of three numerical models (HydroGeoSphere, FEFLOW, and MODFLOW/MT3DMS) to simulate two scenarios. The two scenarios were (1) the experimental situation from Sale et al. (2008) discussed above and (2) a two layer system with an aquifer atop an aquitard solved with the analytical solution from the same study (Chapman and Parker, 2011). The results of their study indicated numerical models can capture field scale diffusion processes given sufficient site data.

2.4 Advection and Dispersion of the CAH

2.4.1 Conceptual Model

Studies conducted by Goodall and Quigley (1977) and Crooks and Quigley (1984) attempted to fit an analytical diffusion-based model to data gathered from cracked clay underlying a municipal landfill in Ontario (Johnson et al., 1989). Both studies resulted in unsatisfactory fits of the models to the data. The poor fits were attributed to

the dominant advective forces through the cracks, which were not accounted for by the models. In this section, models are presented that simulate enhanced transport by accounting for flow through cracks in low permeability media. Conceptually, the transport of dissolved contaminants by advection through cracks results in contaminant being distributed and stored deeper within the low permeability layer than if diffusion was the only relevant transport process .

2.4.2 Analytical Model

Rowe and Booker (1990) used an analytical model to examine transport through a cracked clay landfill liner from the Ontario municipal landfill studied by Goodall and Quigley (1977) and Crooks and Quigley (1984). Previously the authors had determined in reviewing the literature that one of the major assumptions used in selecting clay liners to contain landfill waste, that unweathered till was uncracked, was invalid (Rowe and Booker, 1990). Rowe and Booker (1990) found evidence that unweathered till could in fact be cracked to extensive depths, which would allow for contaminant transport. Rowe and Booker (1990) developed a model that assumed 1-D contaminant transport in the cracks and 2-D diffusion into the surrounding porous medium. The parameters considered by the model included pool height, concentration, crack depth, porosity, crack spacing, and crack aperture. The processes modeled included diffusion, retardation, and hydrodynamic dispersion. The crack spacings ranged from 0.5 to 5 meters, and the apertures ranged from 4 to 9 μm. The results of the analytical model focused on quantifying the effect of crack spacing and Rowe and Booker (1990) concluded that even if the bulk hydraulic conductivity is known, crack density can significantly impact arrival

time to an underlying aquifer. This result suggests that bulk hydraulic conductivity is not a good measure of contaminant transport. Rowe and Booker (1990) also found that the concentration of contaminant reaching the aquifer was very sensitive to porosity and the depth of the cracks.

Ciahn and Tyner (2011) developed a 2-D radial analytical solution for solute transport within a macropore matrix system assuming transverse diffusion and advection of contaminants in high permeability matrices to be the primary transport mechanism~~,~~. Their research focused on a small conceptual model of field scale back diffusion. The goal of their research was to determine analytical solutions for three boundary conditions which would be validated based on previously published data. These were: (1) instantaneous release of solute into a macropore, (2) a constant concentration of solute at the top of the macropore, and (3) a pulse release of solute into the macropore (Cihan and Tyner, 2011). The solutions generated by Cihan and Tyner (2011) assume solute transport at the macropore level is governed exclusively by advection, and solute transport within the matrix is governed exclusively by radial diffusion. Cihan and Tyner (2011) began with Equations 2.7 and 2.8:

$$R_m \frac{\partial C_m}{\partial t} = -v_m \frac{\partial C_m}{\partial z} + \frac{2\theta_a D_a \partial C_a}{r_m \theta_m \partial_r}\Big|_{r=r_m} \quad \text{Equation 2.7}$$

$$R_a \frac{\partial C_a}{\partial t} = \frac{D_a}{r}\frac{\partial}{\partial_r}\left(r\frac{\partial C_a}{\partial r}\right) \quad \text{Equation 2.8}$$

and through application of equations describing boundary conditions (1), (2), and (3) above, produced solutions. The analytical solutions were then compared with

experimental data. The solutions predicted the experimental data well, although accuracy was found to be dependent upon column length.

2.4.3 Numerical Model

A numerical model developed by Grisak and Pickens (1980) used an advective-dispersive transport model to simulate dissolved solute transport in cracked media. Grisak and Pickens (1980) analyzed the impact of different parameters on concentration histories and concentration profiles of solutes in a crack. Important parameters were aperture size, water velocity, porosity, and the distribution coefficient. Their conceptual model included mobile water in high permeability cracks and immobile water in the low permeability matrix surrounding the crack. The model included three major principles, (1) diffusion of the solute into the low permeability matrix from the high permeability crack (2) advection and dispersion due to flow in the crack and (3) linear equilibrium sorption in the matrix.

Models developed prior to the Grisak and Pickens (1980) model emphasized the total effect of cracks on the effective permeability, ignoring the interaction between the high and low permeability matrixes. The dominant transport mechanism in the low permeability no flow matrix is diffusion and the dominant transport mechanisms in the high permeability cracks are advection and dispersion. The crack was modeled as shown in Figure 2.4.

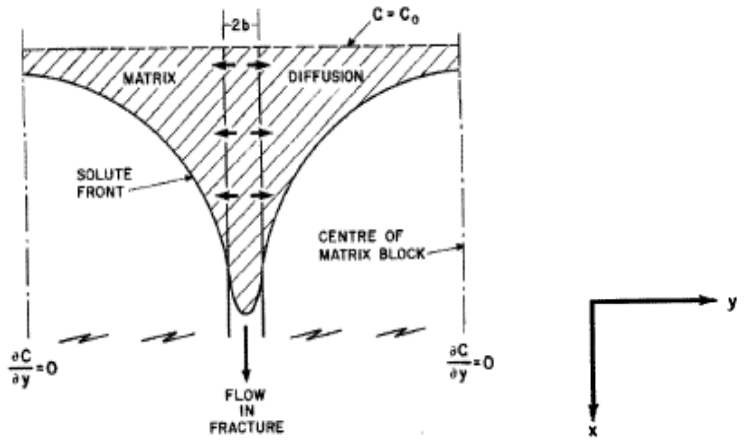

Figure 2-D: Conceptual model of crack used in simulations (Grisak and Pickens, 1980)

A constant source C_0 was maintained at the upper boundary, with a zero concentration gradient at the center of matrix blocks. Assuming a constant concentration of $C=C_0$ at the upper boundary (x=0) would simulate the effect of having pooled DNAPL atop a low permeability lense. The hashed area shows the diffusion of the contaminant into the low permeability matrix surrounding the crack. The model allows for solute to back diffuse out of the matrix into the flowing crack depending on the concentration gradient.

The effect of diffusion within the matrix was quantified by plotting breakthrough curves of the relative concentration (C/C_0) at x=-0.76 m for diffusion coefficients ranging between 0.0 cm^2/s to 10^{-6} cm^2/s. As the diffusion coefficients increased the effect of matrix diffusion became more pronounced. The authors theorized that if the upper boundary condition of $C=C_0$ was replaced with a condition of C=0 the solute would diffuse out of the matrix into the crack. To quantify the impact of aperture size on solute mass transfer a constant velocity in the crack was assumed for a variety of apertures (Grisak and Pickens, 1980). Reducing the aperture size reduces the quantity of solute

transported in the crack and increases the relative amount of solute that enters the matrix, since for a given diffusion coefficient, the mass flux of solute into the matrix is controlled by the concentration gradient only. When the aperture size is decreased the fraction of solute transported within the crack is decreased while the fraction of solute diffused into the matrix is increased (Grisak and Pickens, 1980). Increasing the velocity in the crack increases the solute flux. Higher velocities produced earlier breakthrough; however matrix diffusion became a significant factor after a short time in all scenarios (Grisak and Pickens, 1980). Varying the matrix porosity produced the intuitive result that larger matrix porosities resulted in greater solute transport into the matrix (Grisak and Pickens, 1980). The sorption coefficient, K_d, which quantifies the relationship between dissolved and sorbed contaminant concentrations was varied in the matrix only. The larger the K_d the greater the solute flux into the matrix (Grisak and Pickens, 1980).

2.5 Advection of the DNAPL into Cracks

As will be discussed below, evidence from both the laboratory and the field, as well as modeling analyses, suggest that DNAPL sitting atop a cracked low permeability layer can enter the cracks when the entry pressure is exceeded. Diffusion into the low permeability matrix will then occur, as the DNAPL dissolves from the crack. As the DNAPL mass is reduced due to this dissolution, it will be replenished by the pool.

2.5.1 Evidence and Conceptual Model

The laboratory experiment conducted by O'Hara et al. (2000) which examined fracture flow in laboratory columns found that between 5 and 15% of cracks contribute to

DNAPL flow, and all other cracks could contribute to CAH advection (O'Hara et al., 2000).

Hinsby et al. (1996) studied a clay rich till deposit located near Skaelskor, Denmark. The samples were taken between 2 and 2.5 meters below land surface. The study reports crack values using four methods: (1) hydraulic data, (2) solute transport data, (3) colloid transport data, and (4) measurements of nonwetting fluid entry pressure for a DNAPL, creosote. Cracks were identified by grey/brown halos which surrounded the cracks, and a sample was excavated using hand tools in accordance with Jorgensen and Spliid (1992) and Jorgensen and Foged (1994).

In method (4), creosote was added to the soil and a picture of a sample cross section is shown below in Figure 2.5 with a cartoon showing the magnification of creosote distribution shown in Figure 2.6.

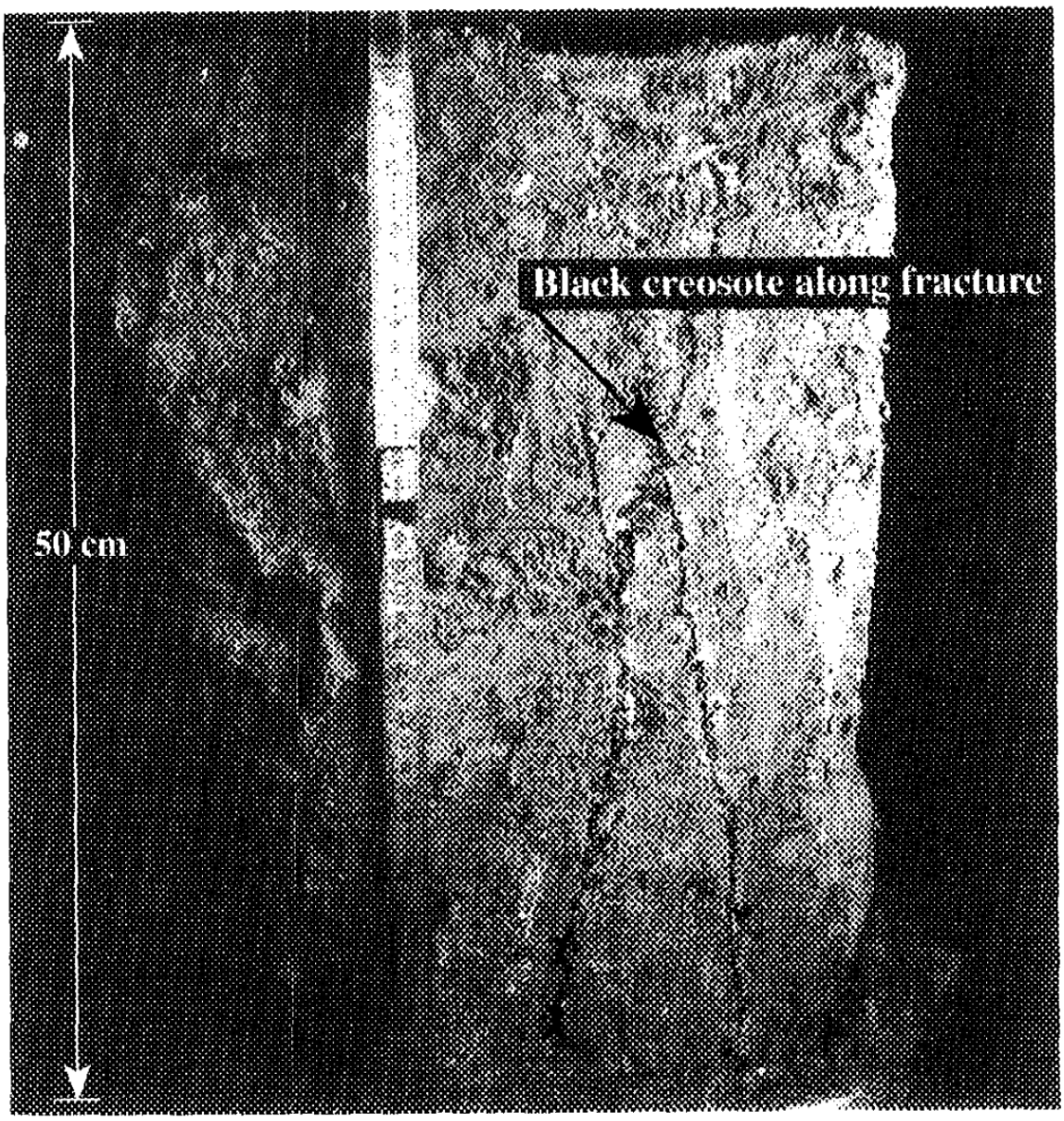

Figure 2-E: Creosote stains in crack (Hinsby et al. 1996)

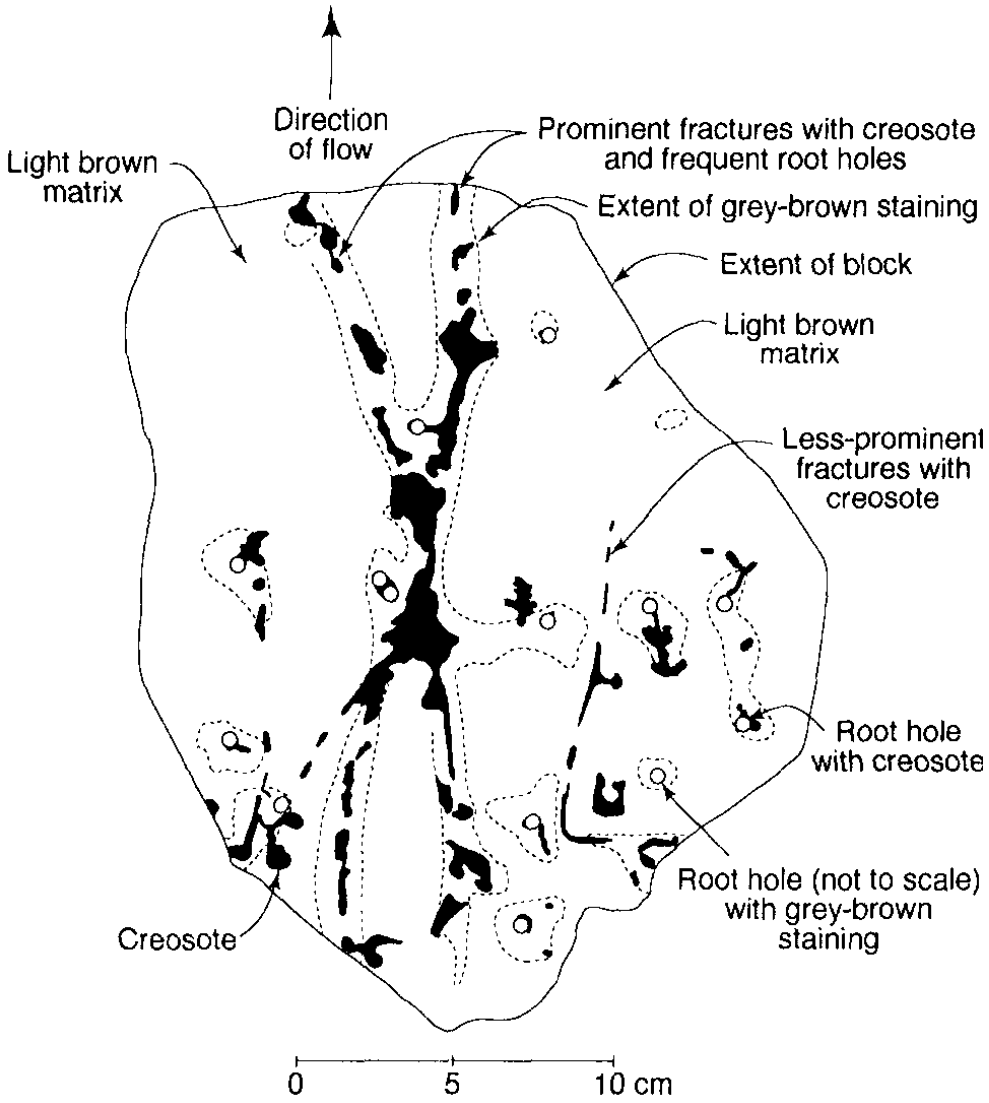

Figure 2-F: Magnification of creosote distribution in crack (Hinsby et al. 1996)

The experiment proved that under pressure highly viscous DNAPLs will enter the clay matrix. Crack apertures were calculated for method (4) using Equation 2.13 which is based on the entry pressure, P_E, required for creosote to enter the crack:

$$2b = \frac{2\sigma cos\theta}{P_E} \qquad \text{Equation 2.13}$$

Where σ [FL^{-1}]is the interfacial tension and θ [°] is the contact angle. Hinsby et al. (1996) concluded that cracks in low permeability layers may permit downward migration

of contaminants. Crack apertures obtained using method (1) were 35 μm and 56 μm with crack spacing's of 0.05 meters and 0.20 meters, respectively. The crack aperture obtained using method (2) was 58 μm, method (3) was 13 to 120 μm, and method (4) 1 to 94 μm.

Hinsby et al (1994) also ran simulations to fit chloride tracer data from the gathered samples. The solute model, CRAFLUSH, was used to simulate a 2-D cross section of column. CRAFLUSH is a flow and transport analytical solution which approximated a crack as two parallel plates and allows for diffusion into the surrounding matrix. The hydraulic conductivity in the model was fixed at the value observed in the laboratory, $1.1x10^{-6}$ m/sec. Crack spacing was varied until the simulated curves fit the observed data. Two methods were used for curve fitting. The first used the cubic law to determine crack aperture, fixing crack spacing and varying vertical hydraulic conductivity. The second method fixed the crack spacing and varied crack aperture. Both methods yielded approximately the same results for crack aperture, 58 μm. The results from the second method also suggested that crack spacing had little impact upon solute transport. In this experiment, the minimal influence of crack spacing is most likely due to the high velocity of flow in the cracks and the short length of the column used in the experiment. In decreased flow scenarios the simulations were more sensitive to crack spacing (Hinsby et al., 1996).

2.5.3 Numerical Model

A model of contaminant transport in cracked aquifers was presented by both Mackay and Cherry (1989), and Kueper and McWhorter (1991). These models suggested

DNAPL will enter cracks which provide the least resistance to flow and will continue to flow into the crack until capillary forces impede DNAPL flow. In these cracks some of the DNAPL will form pools at the bottom of cracks, leave residual along the flow path, and enter the surrounding matrix through diffusion. Both studies found that the crack porosities, void space of the crack per total volume of cracked media, are commonly several orders of magnitude less than most granular aquifers, and therefore little DNAPL can be stored in the cracks. However, this also means flow in cracks can allow for widespread migration of contaminants. A revised model was proposed in Parker et al. (1994; 1997) which demonstrated that the ability of the matrix to store the dissolved DNAPL exceeds the ability of the crack to store the DNAPL. Once the DNAPL enters the crack it is surrounded by a thin layer of water, resulting in a large DNAPL/water interfacial area relative to the DNAPL volume. This allows for a large quantity of the DNAPL to dissolve even though many DNAPLs have relatively low solubilities. Once dissolved, the contaminant will move based on concentration gradients potentially driving the contaminant further into the surrounding matrix.

The model proposed by Parker et al. (1994) for immiscible organic liquids in cracked porous media included the effects of diffusion on the persistence of organic liquids in the cracks. The model takes into account the very high DNAPL surface area to volume ratio, which allows for fast diffusion at the NAPL/water interface. The surface area of NAPL in cracks is large compared to the surface area of a pool atop a low permeability layer. The layer of water surrounding the DNAPL is assumed to instantaneously reach solubility and a chemical concentration gradient will be established with the surrounding matrix. As the DNAPL in the cracks dissolves and diffuses into the

matrix, it is replenished by the DNAPL pool sitting atop the low permeability layer. Eventually, the DNAPL in the cracks will become disconnected ganglia as the height of the DNAPL pool (and therefore, the pressure) decreases and the effects of diffusion are more pronounced (Parker et al., 1994). Mass transfer from the DNAPL to the immobile pore water is included in the Parker et al. (1994) model. The model accounts for reduction in the volume of immiscible DNAPL, thereby reducing the maximum penetration depth. Finally when all or most DNAPL dissolves, the CAH continues to migrate into the matrix as long as the concentration gradients favor this migration. When the pool is no longer atop the low permeability layer and clean water is passing over the cracks contaminants will be removed from the matrix by back diffusion. CAH removal will be controlled by diffusion and desorption from the matrix solids and pore water. The time required for the above processes is dependent upon the properties of the DNAPL, geologic material, and quantity of DNAPL (Parker et al., 1994).

Parker et al. (1994) also studied the impact of crack spacing on contaminant flux. Previous models had assumed a single crack in an infinite porous medium which allows large concentration gradients to form. In reality concentration gradients will form around all cracks, and when the concentration gradients compete, the diffusion and mass flux from crack surfaces will decrease. The time when diffusion profiles will meet between cracks after a release of DNAPL is dependent upon the distance between cracks, DNAPL properties, and matrix properties. Medium to narrow aperture size, high aqueous solubility, large porosity, and high sorption capacity of the matrix were shown to enhance the rate of the NAPL dissolution (Parker et al., 1994).

Kueper and McWhorter (1991) examined conditions for DNAPL transport into cracks. In their equations it is assumed the matrix is initially fully saturated with water, and that water is the wetting fluid and the DNAPL is the nonwetting fluid.

Capillary pressure (P_C) is defined as the difference in pressure between that in the nonwetting fluid (P_{NW}) and that in the wetting fluid (P_W) as shown in Equation 2.9.

$$P_C = P_{NW} + P_W \qquad \text{Equation 2.9}$$

As previously stated, for the DNAPL to enter the clay matrix the capillary pressure at the top of the crack must exceed the entry pressure (P_E) of the DNAPL. Two equations will predict P_E, Equation 2.10 is for irregular crack patterns approximated by two parallel plates, and Equation 2.11 is for circular cracks.

$$P_E = \frac{2\sigma cos\theta}{2b} \text{ parallell plates} \qquad \text{Equation 2.10}$$

$$P_E = \frac{4\sigma cos\theta}{2b} \text{ circular} \qquad \text{Equation 2.11}$$

σ [FL^{-1}] is the interfacial tension between the DNAPL and the water, θ [-] is the contact angle measured through the wetting phase, and 2b [L] is the crack aperture. From the equations it is noted that DNAPL entry pressure is inversely proportional to crack aperture; that is, larger crack apertures require lower P_E for DNAPL entry into the crack. In reality the entry pressure will lie in between the entry pressure predicted by Equations 2.10 and 2.11. Figure 2.7 shows two possible idealizations of a rough walled crack.

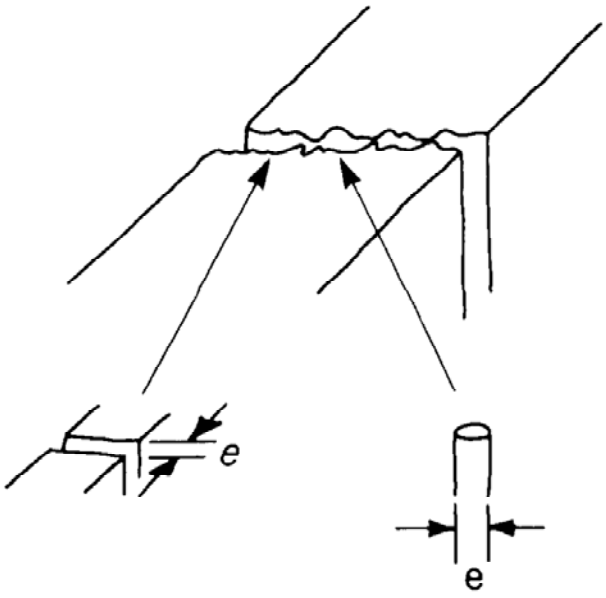

Figure 2-G: Rough crack and two idealizations (Kueper and McWhorter, 1991)

Cracks in nature are generally elongated and irregular, therefore Equation 2.9, which results in a lower entry pressure, will be used for calculations. Using a lower entry pressure is conservative. The DNAPL pool height (H_D) required to create a given entry pressure is given by equation 2.12:

$$H_D = \frac{2\sigma}{\Delta\rho g 2b} \qquad \text{Equation 2.12}$$

where $\Delta\rho$ [ML^{-3}] is the density difference between water and the DNAPL. Equation 2.12 displays an inverse relationship between aperture width and the pool height required for DNAPL entry. The Kueper and McWhorter (1991) model also indicated that DNAPL transport through a cracked aquitard increased with downward water gradients and decreased with upward water gradients across the aquitard. (Kueper and McWhorter, 1991).

Reynolds and Kueper (2002) examined the effects of crack aperture, matrix porosity, and matrix organic carbon on the migration of five DNAPLs using numerical simulations. The study found that aperture is the most important factor impacting migration of DNAPLs in cracks. Particularly in large cracks matrix diffusion does not retard the rate of DNAPL migration. By increasing the crack aperture from 15 μm to 50 μm there was a 20 fold increase in the rate of DNAPL migration downward (Reynolds and Kueper, 2002).

Murphy and Thomson (1993) developed a dynamic two-dimensional two-phase flow model for a single aperture. The system was a finite volume implementation of the cubic rule, Equation 2.1, and assumes incompressible flow between parallel plates. Esposito and Thomson (1999) extended the two phase crack flow model developed by Murphy and Thomson (1993). Their numerical model includes transient two-phase flow, non-equilibrium dissolution, advective-dispersive transport in the crack, and three-dimensional matrix diffusion (Esposito and Thomson, 1999). The authors were investigating (1) the role dissolution and diffusion have on DNAPL disappearance and (2) how changing flushing rates affect DNAPL mass removal. The model approximated two phase flow in a single crack as parallel plate flow. Apertures are generally rough and can vary in width considerably, therefore Esposito and Thomson (1999) created log normal aperture distributions using an algorithm developed by Robin (1991). This allows the domain for the model to be a crack network with varying apertures incorporating the narrowing of cracks with depth. Figure 2.8 is an example of an Esposito model domain (2D cross section).

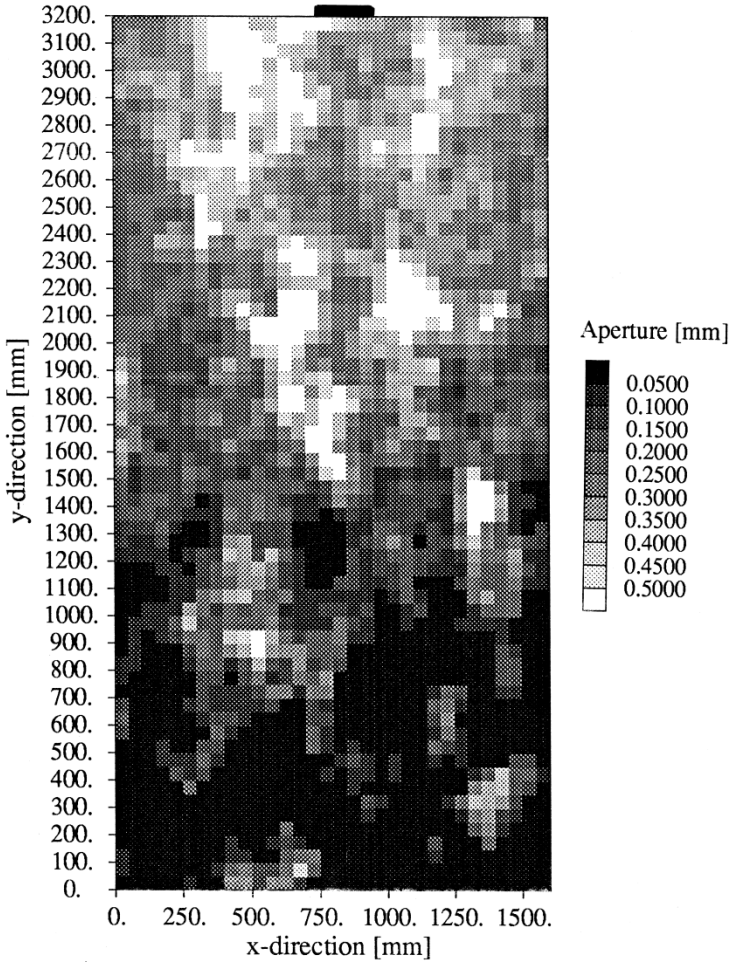

Figure 2-H: Variable aperture model domain (Esposito and Thomson, 1999)

Figure 2.8 has an average aperture value of 210 μm and was used to investigate the role of dissolution and diffusion on DNAPL disappearance. As seen above the domain is relatively small and therefore it was necessary to assume that the size of the control volume (shown above) sufficiently accounted for aperture variations (Esposito and Thomson, 1999). Also, the model does not account for large scale heterogeneities in the media.

The authors used three materials for their simulations, Clay 1 which had a porosity of 0.35 and a fraction of organic carbon (f_{oc}) of 0.01, Clay 2 which had a

porosity of 0.55 and a f_{oc} of 0.005, and shale/sandstone which had a porosity of 0.10 and a f_{oc} of 0.002. The retardation coefficient of Clay1 and 2 was 6.8 while the Shale/Sandstone was 7.0. Clay 1 and 2 used the same diffusion coefficient while the Shale/Sandstone used a much lower coefficient (Esposito and Thomson, 1999).

The first investigation compared the time it took for the DNAPL TCE to travel 0.13 and 0.43 meters in the porous media. In Clay 1, it took 64.8 years, in Clay 2, 22.0 years, and in the Shale/Sandstone it took 486.1 years (Esposito and Thomson, 1999). These results mean a high porosity and low f_{oc} allow for faster DNAPL travel. A smaller porosity and diffusion coefficient in the Sandstone/Shale impaired downward movement but also prevented significant mass movement into the surrounding matrix. These findings were consistent with the findings in Parker et al. (1994).

The second investigation analyzed the effectiveness of mass removal methods which rely on hydraulic gradients. 20g of the DNAPL was allowed to enter the grid and then three different hydraulic gradients (0.4, 0.04, and 0.004) were used to flush the DNAPL. The model assumed mass removal began immediately following the DNAPL release, which is very optimistic since most spills are not detected until many years after the spill occurred. The time required to remove 99% of the mass ranged from 10 days to several hundred years, which means remediation technologies that use hydraulic gradients (such as pump and treat) may be severely impaired in a cracked clay environment. Further, if the pool of DNAPL remains as a long term source the high concentration gradients surrounding the cracks will drive more contaminant into the surrounding matrix making complete mass removal even more difficult (Esposito and Thomson, 1999).

3. Methodology

3.1 Overview

Cracking in clay is hypothesized to contribute to enhanced diffusion and storage of contaminants in low permeability layers. Cracks are known to form naturally in low permeability layers as a result of natural loading and unloading cycles as well as ~~dessication~~desiccation (McKay and Fredericia, 1995) (Esposito and Thomson, 1999). Recent research has also indicated pooled DNAPL can cause cracks. Pooled DNAPL is hypothesized to then enter the cracks. In this study, a numerical grid is created to simulate a high conductivity sand layer sitting atop a low conductivity clay layer. The results reported in Miniter (2011) are verified, and the transport of TCE is modeled in three scenarios. These scenarios are: (1) transport into uncracked clay, (2) transport of the dissolved TCE into cracked clay, and (3) transport of DNAPL phase TCE into cracked clay. This work is an extension of the work done by Miniter et al. (2011) and will evaluate the impact of cracking on enhanced diffusion and storage into low permeability layers. The model in scenarios (2) and (3) assumes the existence of cracks in the low permeability layers, but does not differentiate between naturally occurring or DNAPL caused cracks.

3.2 General Description

This research assumes a heterogeneous system composed of three media: sand, clay, and cracked clay. A DNAPL source is simulated within a high permeability sand layer atop a low permeability clay layer. The contaminant will be transported into the clay through various transport processes including diffusion, advection of the CAH, and

advection of the DNAPL. In uncracked clay, it is hypothesized the only mechanism of transport of the DNAPL into the clay is diffusion. In cracked clay it is hypothesized the TCE will either advect as a pure phase DNAPL or as dissolved CAH into the cracks. In the cracked clay, the contaminant will then diffuse into the surrounding clay matrix based on concentration gradients. The increase in transport due to cracking will be termed "enhanced diffusion." The enhanced diffusion into the clay could lead to a significant increase of contaminant storage in the clay layer. Figure 3.1 is a conceptual diagram depicting the source zone.

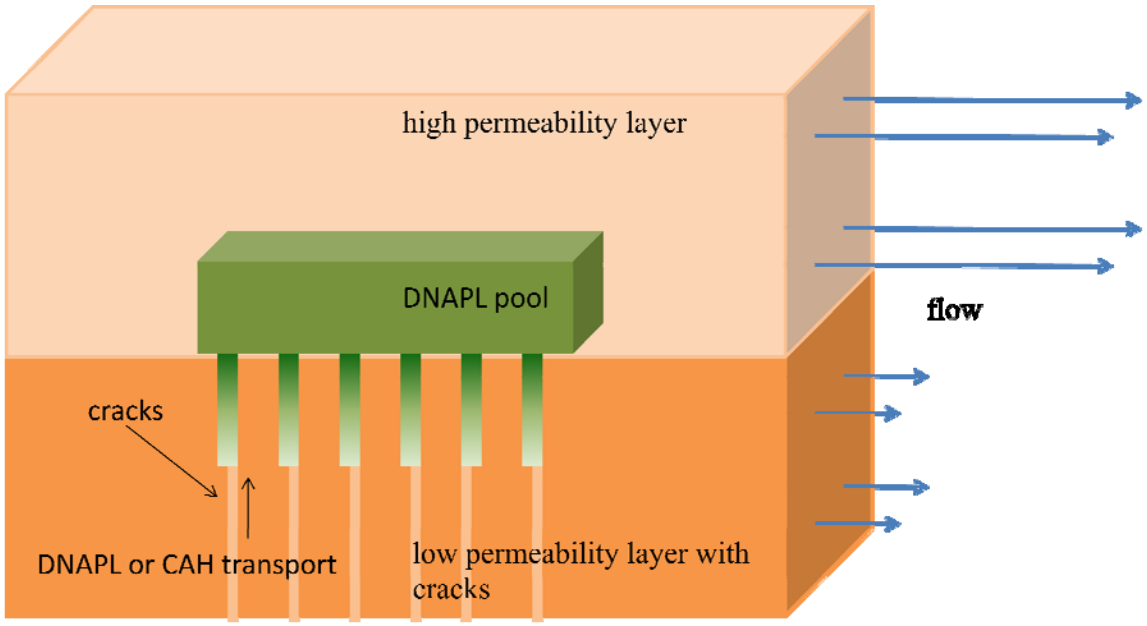

Figure 3-A: Source Zone Conceptual Diagram

Dissolution of the DNAPL into the high flow sand layer will remove much of the DNAPL mass and create a down gradient plume. This plume will result in concentration gradients down gradient of the source zone which will permit further transport by diffusion into the low permeability clay layer. Once the source is removed, it is

hypothesized the CAH will diffuse out of the low permeability clay layer perpetuating the plume at lower concentrations. Monitoring wells placed in the high permeability layer will show the concentration history of the dissolved plume down gradient of the source. Modeling will allow us to quantify the mass stored in the low permeability layer, as well as the down gradient concentration history. Analysis of the model results will provide an increased understanding of the relationship between cracking, mass storage, and plume behavior. Figure 3.2 depicts plume formation and a plume observation point.

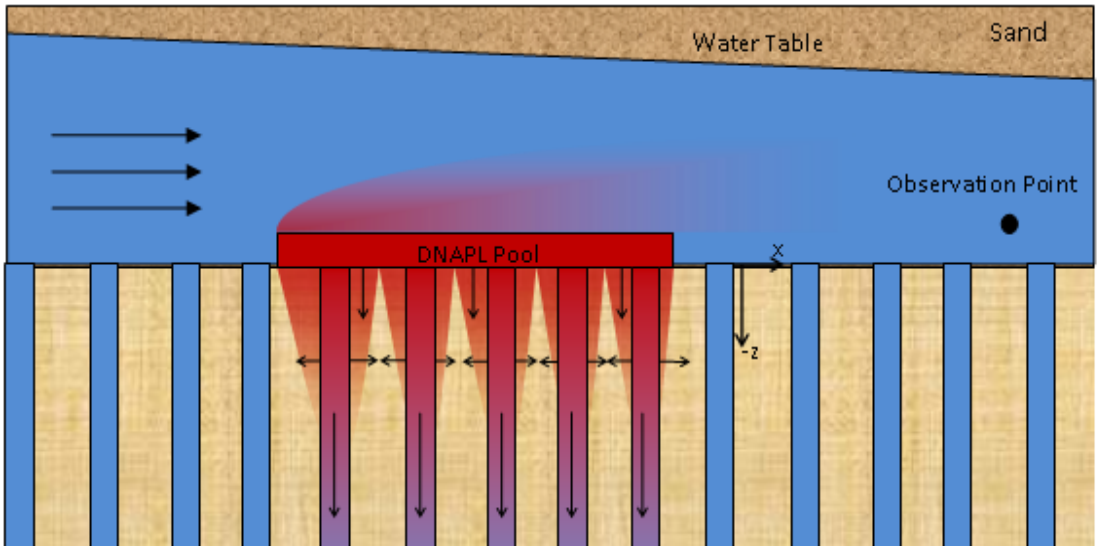

Figure 3-B: Plume Formation and Observation Point Conceptual Diagram

3.2.1 Assumptions

Many key assumptions are required to model contaminant transport in an aquifer system. In general, the subsurface is anisotropic and heterogeneous. This means flow can be significantly different at two different points in the same medium. This model assumes the same hydraulic and chemical properties within each defined layer. The source is assumed to be instantaneously removed, simulating total remediation of

DNAPL mass in the high permeability zone. Further, when modeling the cracks it is necessary to assume uniform aperture, spacing, and depth. When modeling DNAPL transport into the cracks it was assumed the DNAPL has fully penetrated the crack prior to the start of the simulation. Also, to ensure the DNAPL transport is more realistically modeled, at ten years once the source is removed the DNAPL is again assumed to have fully saturated the crack.

In this thesis, we assume cracked clay can be modeled as an equivalent homogeneous anisotropic medium with increased vertical hydraulic conductivity. Figure 3.3 below provides a visual representation of this assumption.

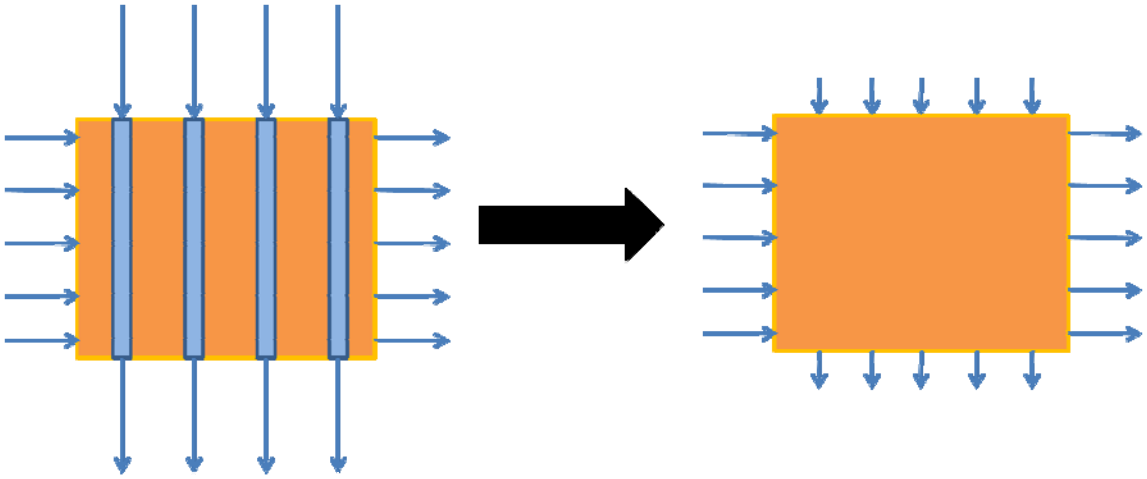

Figure 3-C: Vertical Flow Approximation for Cracking

3.3 Governing Equations

Many of the equations used in the model and for basic calculations are the same equations used by Miniter (2011). For a further explanation of equations consult the work of Minter (2011).

3.3.1 Dissolved Transport

The primary equation governing contaminant transport in porous media is shown below in Equation 3.1:

$$J_{TCE} = \frac{\partial}{\partial x_i}\left(D_{ij}\frac{\partial C}{\partial x_j}\right) - \frac{\partial}{dx_i}(v_i C) - \rho_b \frac{dS}{dt} \qquad \text{Equation 3.1}$$

where J_{TCE} [$ML^{-2}T^{-1}$] is the contaminant flux, x [L] is the distance along the respective Cartesian coordinate axis, C [ML^{-3}] is the concentration of dissolved contaminant, , D_{ij} [L^2T^{-1}] is the hydrodynamic dispersion coefficient tensor, v_i [LT^{-1}] is the linear pore water velocity, ρ_b [ML^{-3}] is the bulk density, and S [ML^{-3}] is the sorbed contaminant. While Equation 3.1 is applied throughout the entire model domain, transport in sand, clay, and cracked clay will vary based on the specific medium's properties.

The hydrodynamic dispersion coefficient combines the effects of mechanical dispersion and diffusion into one term. This relationship is shown in Equation 3.2 (Gupta, 2008):

$$D_{ij} = D_{eff} + D_m \qquad \text{Equation 3.2}$$

D_m is the mechanical dispersion coefficient given by Equation 3.3:

$$D_m = \alpha_{ij} v_i \qquad \text{Equation 3.3}$$

Where α_{ij} [L] is the dispersivity parameter and v_i [LT^{-1}] is the linear pore water velocity. D_{eff} is the effective molecular diffusion coefficient. The effective diffusion coefficient (D_{eff}) is related to the free-solution diffusion coefficient (D_0) shown below in Equation 3.4.

$$D_{eff} = D_o \tau \qquad \text{Equation 3.4}$$

where τ is a tortuosity factor (0<τ<1~~) that~~) that accounts for the hindrance to diffusion through porous media (Gupta, 2008).

Diffusive transport in cracks and into the surrounding matrix is governed by Fick's second law shown below in Equation 3.5 (Johnson et al., 1989).

$$\frac{\partial C}{\partial t} = D_{eff} \frac{\partial^2 C}{\partial x_i^2} \qquad \text{Equation 3.5}$$

Where D_{eff} [L^2T^{-1}] is the effective diffusion coefficient, C [ML^{-3}] is the aqueous concentration, and x_i [L] is the respective Cartesian coordinate. As seen in Equation 3.5, the transport of mass into the clay is determined by the concentration gradients.

TCE, like many other DNAPLs, will readily adsorb to organic material in porous media. As the concentration increases in the flowing groundwater, the mass adsorbed to organic materials will increase proportionally. Sorption may be modeled as a kinetic process, as is shown below in Equation 3.6

$$\rho_b \frac{\partial S}{\partial t} = \theta\alpha(C - k_d S) \qquad \text{Equation 3.6}$$

Where S is the sorbed mass [M], θ [-] is the media porosity, k_d [ML_{water}^{-3}] is the sorption coefficient, and α [T^{-1}] is the first order mass transfer coefficient between the water and solid grains of the aquifer. In this study, sorption is assumed to be negligible (α = 0).

The DNAPL within the cracks will slowly diffuse into the flowing water based on concentration gradients. In order to effectively model DNAPL dissolution, a step function must be used. Equation 3.7 is the differential equation modeling the first order

DNAPL dissolution, and Equation 3.8 is the step function indicating DNAPL dissolution ends when the DNAPL is completely dissolved and no longer present.

$$\rho_{NAPL}\frac{\partial S_{NAPL}}{\partial t} = \beta(C - F) \qquad \text{Equation 3.7}$$

$$F = \begin{cases} C_S & S_{NAPL} > 0 \\ C & S_{NAPL} = 0 \end{cases} \qquad \text{Equation 3.8}$$

Where ρ_{NAPL} [ML^{-3}] is the NAPL density, S_{NAPL} [-] is the NAPL saturation, C_S [ML^{-3}] is the DNAPL solubility in water, β [T^{-1}] is the first order mass transfer coefficient between the DNAPL and the flowing water, and C [ML^{-3}] is the concentration of the dissolved DNAPL. β is determined using the following relationship in Equation 3.9 (Christ et al., 2006):

$$\beta = k_0' \left(\frac{M(t)}{M_0}\right)^{\beta_{Christ}} \qquad \text{Equation 3.9}$$

Where k_0'[T^{-1}] is a fitting parameter, M(t) [M] is the time dependant mass, M_0 [M] is the mass at time zero, and β_{Christ} [-] is a fitting parameter. For this work, β is assumed to be constant, and its value determined by using $\frac{M(t)}{M_0} = 0.5$. Values used from Christ et al. (2006) for k_0' and β_{Christ} are 8.2e-3 d^{-1} and 0.85, respectively.

3.3.2 Cracking

The number of cracks in the clay at the source can be determined using Equation 3.10:

$$c = \left(\frac{L}{2B} + 1\right)\left(\frac{W}{2B} + 1\right) \qquad \text{Equation 3.10}$$

where c [-] is the number of cracks, L [L] is the length of the source zone, W [L] is the width of the source zone, and 2B is the distance between cracks. In order to model advection of DNAPL within the cracks it is necessary to calculate crack volume. The equation for a single crack volume is shown below in Equation 3.11:

$$V_{crack} = hb^2\pi \qquad \text{Equation 3.11}$$

Where h [L] is the crack depth and b [L] is the crack radius. The surface area of the crack, where diffusion will occur, is given by Equation 3.12:

$$SA_{crack} = h2b\pi \qquad \text{Equation 3.12}$$

where SA is the crack surface area [L^2]. The volume of NAPL in a crack is given by Equation 3.13:

$$V_{NAPL} = V_{crack}(1 - r_{sw}) \qquad \text{Equation 3.13}$$

Where V_{NAPL} [L^3] is the volume of NAPL in the crack and r_{sw} [-] is the residual saturation of water. The water residual saturation is the fraction of water in the crack which will not be displaced by DNAPL. The residual water saturation can range from 0 to 1, and can be determined for a particular media based on relative permeability curves. In this thesis, the residual water saturation is assumed to be 0.1.

Within the model, modeling individual cracks proved infeasible; therefore, as noted earlier, flow in cracks was simulated as increased vertical conductivity. In order to model the DNAPL within the cracks it is assumed that the DNAPL fully penetrates the cracks instantaneously. With this assumption the total volume of DNAPL entering the

cracks can be calculated and distributed within the matrix. Equation 3.14 gives the total volume of DNAPL.

$$V_{NAPLtotal} = V_{NAPL}c \qquad \text{Equation 3.14}$$

The DNAPL will be simulated as being evenly distributed throughout the areas containing cracks with saturation S_{NAPL}, given below in Equation 3.15:

$$V_{cracksource}S_{NAPL} = \frac{V_{NAPLtotal}}{\theta} \qquad \text{Equation 3.15}$$

Where $V_{cracksource}$ [L^3] is the volume of the aquifer containing cracks, S_{NAPL} [-] is the DNAPL saturation (volume of DNAPL per volume of void). Figure 3.4 is a simple conceptual model of DNAPL distribution at a residual saturation. The DNAPL is shown in red, the soil grains in dark blue, and the water in light blue.

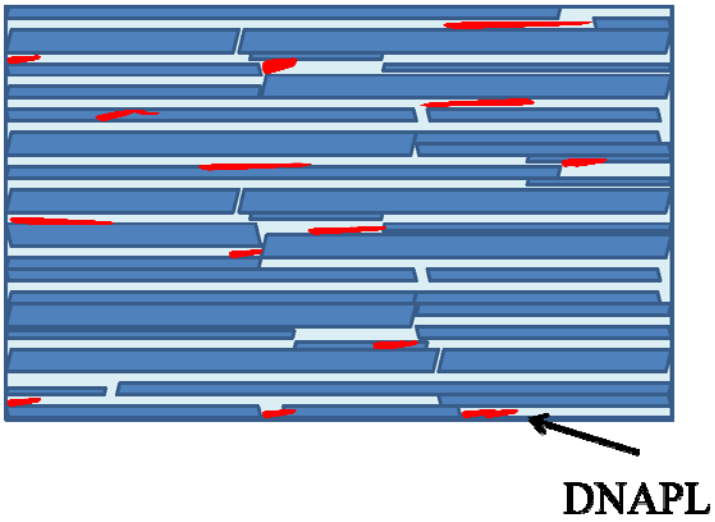

Figure 3-D: DNAPL in Cracks Approximated as Saturation

3.4 Model Implementation

The effect of cracking was examined using a program called Ground Water Modeling System (GMS). The scenarios discussed below are hypothesized to demonstrate the impact of cracking on down gradient contaminant plume concentrations. The contaminant modeled in these simulations is TCE.

3.4.1 Model Scenarios

Three distinct scenarios are considered and evaluated using GMS. The three scenarios are evaluated using the same baseline conditions for hydraulic gradient, DNAPL pool position, pool area, source exposure/removal monitoring time, and monitoring well position. The three scenarios are listed below and will be referred to by scenario number for the remainder of this thesis.

1. Transport of the CAH into an uncracked clay matrix (transport assumed to be governed by diffusion only)
2. Transport of the dissolved CAH into a cracked clay matrix (transport assumed to be governed by advection and diffusion)
3. Transport of the DNAPL and diffusion of the CAH into a cracked clay matrix (transport assumed to be governed by diffusion and advection of the CAH coupled with dissolution of the DNAPL)

Figure 3.5 provides a conceptual model of each scenario beneath the source zone. Only one crack is shown for scenarios 2 and 3.

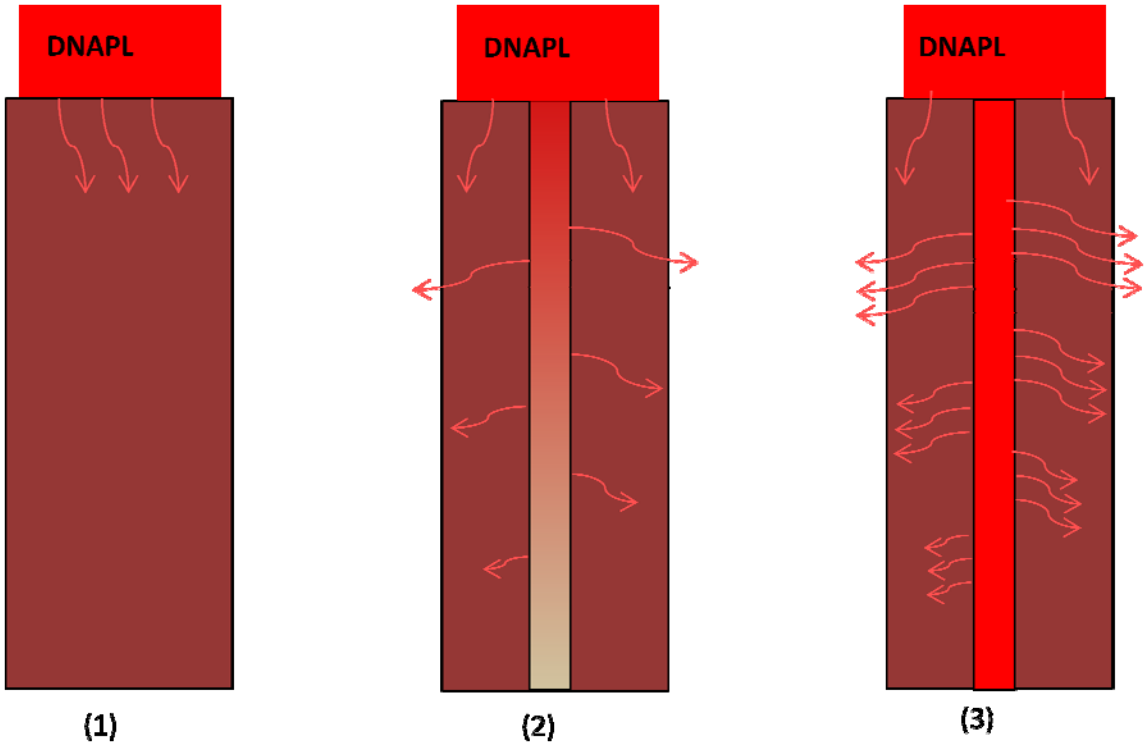

Figure 3-E: Conceptual Diagram of Contaminant Transport Beneath a Source Zone for Scenarios 1-3

3.4.1 Ground Water Modeling System

GMS was used to evaluate the impact of cracking on down gradient plume concentrations. Three GMS modeling packages were used in this work, MODFLOW, MODPATH, and RT3D. A three dimensional grid was created with a length of 100m, a width of 70m, and a total depth of 14m. Each cell in the grid was a 1 meter cube. The high permeability sand layer was 6m thick atop a 6m low permeability clay layer. The clay layer overlaid a 2m high permeability sand layer. The 2m sand layer was needed to avoid having a no-flow boundary condition at the bottom of the clay layer. Within the low permeability layer, a 192m^2 cracked clay zone was emplaced for scenarios 2 and 3. For more detail on the numerical domain, see Appendix A. Figure 3.6 is a conceptual

diagram depicting the media properties used in scenario one (Figure 3.6(a)) and in scenarios 2 and 3 (Figure 3.6(b)). The darkened area in Figure 3.6b represents the cracked area beneath the source.

GMS was used to evaluate the impact of cracking on down gradient plume concentrations. Three GMS modeling packages were used in this work, MODFLOW, MODPATH, and RT3D. A three dimensional grid was created with a length of 100m, a width of 70m, and a total depth of 14m. Each cell in the grid was a 1 meter cube. The high permeability sand layer was 6m thick atop a 6m low permeability clay layer. The clay layer overlaid a 2m high permeability sand layer. The 2m sand layer was needed to avoid having a no-flow boundary condition at the bottom of the clay layer. Within the low permeability layer, a 192m^2 cracked clay zone was emplaced for scenarios 2 and 3. For more detail on the numerical domain, see Appendix A. Figure 3.6 is a conceptual diagram depicting the media properties used in scenario one (Figure 3.6(a)) and in scenarios 2 and 3 (Figure 3.6(b)). The darkened area in Figure 3.6b represents the cracked area beneath the source.

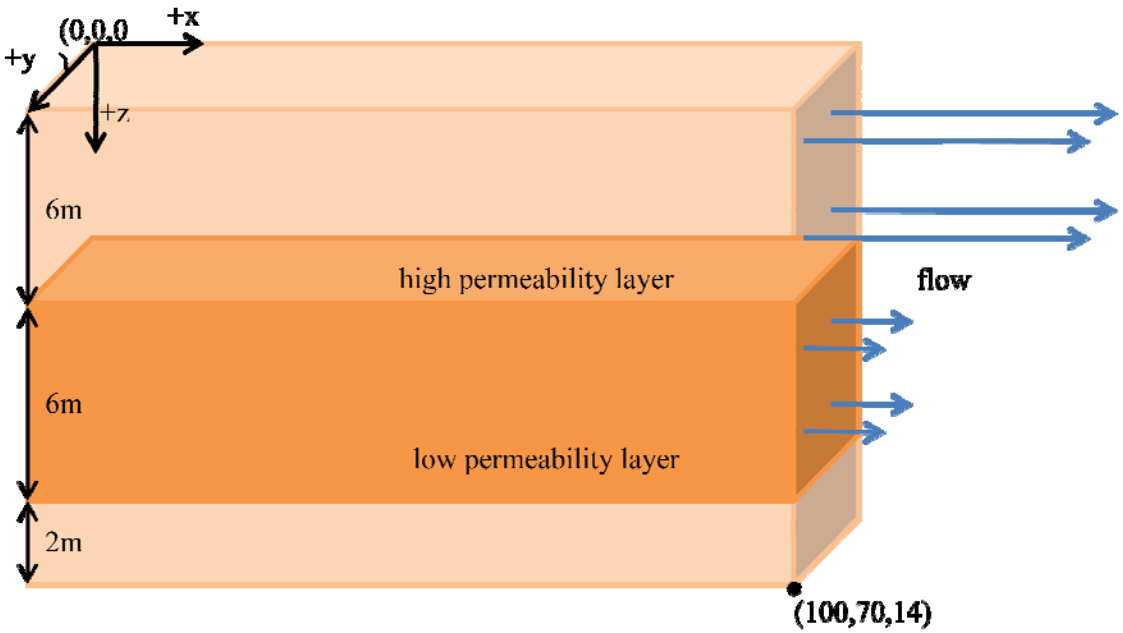

(a)

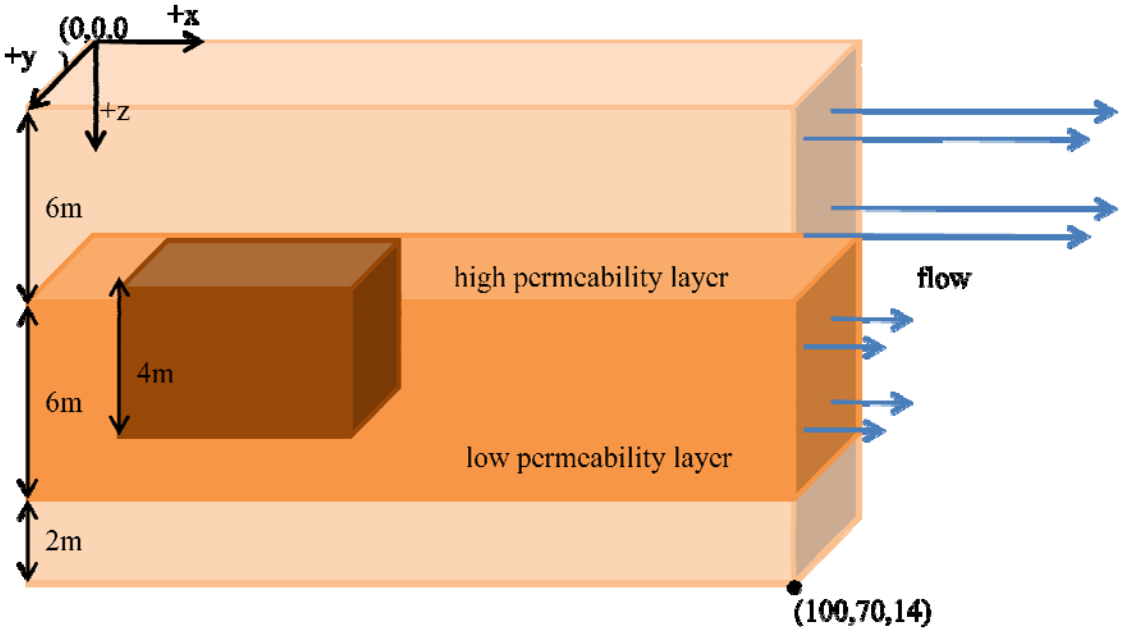

(b)

Figure 3-F: Model used for (a) Scenario 1 – uncracked clay (b) Scenarios 2 and 3 – cracked clay

As a first step in modeling contaminant transport, initial flow conditions must be established. The aquifer was assumed to be unconfined, and a horizontal hydraulic gradient of 1m/100m was created by setting the head at the left and right side boundaries of the domain at 14.5 and 13.5m, respectively. A vertical hydraulic gradient of 0.5m/14m was established by setting the bottom heads at the left and right hand boundaries to 14.0m and 13.0m, respectively. Values of the vertical and horizontal hydraulic conductivity, longitudinal dispersivity, and porosity were assigned to the sand, clay, and cracked clay as shown below in Table 3.1.

Table 3-1: Parameter Values Input into MODFLOW

	Sand	Clay	Cracked Clay
Horizontal K_h (m/d)	17.28	4.32×10^{-5}	4.32×10^{-5}
Vertical K_v (m/d)	1.728	4.32×10^{-6}	4.32×10^{-4}
Longitudinal Dispersivity (m)	1.0	1.0×10^{-4}	1.0×10^{-4}
Porosity (θ)	0.35	0.43	0.487

Miniter et al. (2011)

MODFLOW was used to compute the steady state flow heads for each of the three scenarios based on the system parameters in Table 3-1. Three monitoring wells were placed 50m down gradient of the source to monitor plume concentrations. The locations of the monitoring wells are shown below in Figure 3.7 as black dots. One well was placed in the sand layer, one at the clay/sand interface, and one in the clay. A typical MODFLOW output showing hydraulic heads throughout the model domain is shown below in Figure 3.7.

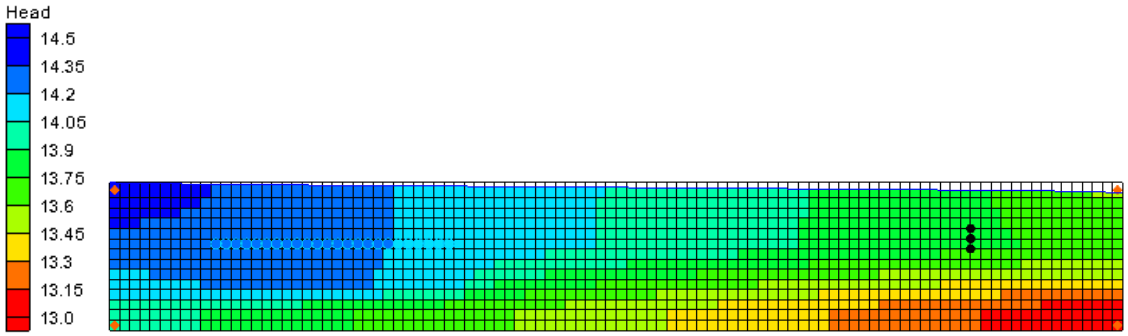

Figure 3-G: MODFLOW Output Along a Longitudinal Cross Section

MODPATH can then be used to evaluate the flow of particles through the system to help visualize flow conditions and identify stagnation points.

The MODFLOW solution is then read by RT3D which then simulates the advection, dispersion, sorption, and diffusion of the contaminant through the domain. Two periods were used to simulate a DNAPL release into the subsurface. In the first ten year period, a 192m^2 DNAPL pool source was simulated by holding the concentration of cells at a constant value for 10 years. After this ten year period, it was assumed the source is remediated, and the constant concentration source was removed. The contaminants were then transported out of the low permeability layer based on concentration gradients. The model was then run for an additional 40 years to examine the effect of this back diffusion on down gradient plume concentrations as well as the DNAPL dissolution into the aquifer.

In RT3D a user defined transport package written by Dr. Junqi Huang (Personal communication, 2011) was used. The transport package requires the user to define various parameter values for the contaminant and media. These parameters are the bulk density of the media, the sorption coefficient of the media, the mass transfer coefficient

from the dissolved phase to the soil, solubility of the DNAPL, bulk density of the DNAPL, the mass transfer coefficient describing the dissolution of the DNAPL to the surrounding water, and the diffusion coefficient in the media. The values used for the different media are shown below in Table 3.2 and the contaminant properties are shown below in Table 3.3.

Table 3-2: RT3D Media Values

Media	Sand	Clay	Cracked Clay
Bulk Density (ρ_b) (kg-m^{-3})	1722	1499	1349
Sorption Constant (K_d) (mg-L^{-1})	65.4	1908	1908
Diffusion Coefficient (D_{eff}) (cm^2-s $^{-1}$)	0.0	8.64 x 10^{-6}	8.64 x 10^{-6}

(Miniter, 2011)

Table 3-3: RT3D Chemical Values

Media	TCE
Bulk Density (ρ_b) (kg-m^{-3})	1460
NAPL Solubility (C_S) (mg-L^{-1})	110[(1)]
First Order Sorption Rate Constant (α) (d^{-1})	0.0
First Order NAPL Dissolution Rate Constant (β) (d^{-1})	0.00445[(2)]

[(1)]10% of TCE solubility (Miniter, 2011), [(2)] (Christ et al., 2006)

Sorption is not examined in this ~~work,~~work; therefore the first order sorption rate constant equal used is zero, effectively removing all sorption processes. Using Equations 3.14 and 3.15 the NAPL saturation is determined for scenario 3. For these scenarios it is

assumed the average crack aperture is 150 µm, the cracks are 0.03m apart, and extend 4m in depth. Given these values it is assumed there are 214,401 cracks in the 192 m^2 source zone. The DNAPL saturation is set at $6.62x10^{-5}$ for scenario 3 at two times, 0 and ten years. The saturation cannot be held constant throughout the first ten years, therefore it is reset at ten years when the source has been removed to more realistically simulate DNAPL recharge into the cracks.

3.5 Results Analysis

Two methods were used to quantify the effect of cracks on DNAPL contaminant fate and transport: a mass analysis and examination of concentration versus ~~time breakthrough~~time breakthrough curves at down gradient locations. The first method, a mass analysis, quantified the total mass stored in the low permeability layer. Mass could be stored in three ways: in the aqueous phase, sorbed to the soil solids (though in this study, sorption is considered negligible), and in Scenario 3, in the NAPL phase. The mass in the three scenarios was compared at three points in time: at the start of the simulation, immediately after the source is removed, and 40 years after the source has been removed.

The second method, used by Miniter et al. (2011), examined predicted concentrations at the observation wells. Typically, it will take a relatively short time for dissolved contaminant from the source to reach the observation well. After the source is removed, the concentration at a given observation well will decline. It has been observed that, with DNAPLs, the concentration rapidly declines when the source is removed, followed by the persistence of low levels for extended periods of time. This slow decline

at long periods of time is termed "tailing" (Parker et al., 2008). This concentration history can then be used to determine the time required for aqueous concentrations to reach the regulatory MCL (5 ug/L for TCE).

It is also possible to describe the breakthrough curve by its first moment. The first moment measures the center of mass of a distribution. The higher the value of the first moment of a breakthrough curve at a given monitoring well, the longer contamination is persisting at that monitoring well. A high value for the first moment may be indicative of tailing. It is hypothesized that both the first moment and the time to attain MCLs will increase significantly from Scenario 1 to 3.

In this study, the first moment of breakthrough curves was determined for Scenarios 1-3.

In order to calculate the first moment, the area under the breakthrough curve was calculated using Equation 3.16.

$$\text{area} = \sum_{i=0}^{i_{max}-1} \left[\frac{c(t_{i+1})+c(t_i)}{2}\right](t_{i+1} - t_i) \qquad \text{Equation 3.16}$$

where c(t) [mg-L^{-1}] is the concentration output from GMS at time t_i [T].

The discrete residence time density function ($f(t_i)$) is then determined for each discrete concentration value using Equation 3.17.

$$f(t_i) = \frac{c(t_i)}{\text{area}} \qquad \text{Equation 3.17}$$

The first moment is then calculated using Equation 3.18.

$$\bar{t}_{RTD} = \sum_{i=0}^{i_{max}-1} \left[\frac{(t_i+t_{i+1})}{2}\right]\left[\frac{f(t_i)+f(t_{i+1})}{2}\right](t_{i+1} - t_i) \qquad \text{Equation 3.18}$$

where $\bar{t}_{RTD}$ [T] is the mean residence time or first moment (Clark, 2009).

3.5.1 Sensitivity Analysis

A sensitivity analysis was used to determine those parameters which, when varied, have the most impact on down gradient plume concentrations. Scenario 3 was be used in the simulations to quantify the impact of different model parameters. The sensitivity analysis focused on the impact of varying the first order NAPL dissolution rate constant (β) and the vertical hydraulic conductivity (K_v) below the source. β was varied by two orders of magnitude in order to determine the effect of DNAPL dissolution. As β increases or decreased, the concentration at the source should also increase or decrease in accordance with Equations 3.7 and 3.8. The vertical conductivity, K_v, was also varied by two orders of magnitude to determine the impact of increased and decreased vertical flow at the source zone. Table 3.4 below lists baseline values for β and K_v as well as the values used in this sensitivity analysis.

Table 3-4: Sensitivity Analysis Values

	Lower Sensitivity Analysis ~~Vaslue~~Value	Baseline Value	Upper Sensitivity Analysis Value
β (d^{-1})	4.45E-5	0.00445	0.445
K_v ($m\text{-}d^{-1}$)	4.32E-6	0.000432	0.0432

The effect of changing β and Kv will be quantified by: (1) time to reach MCL at down gradient wells, (2) down gradient well breakthrough curve first moment, and (3) comparison of mass of contaminant stored in the low permeability layer immediately following source removal (10 years) and at the conclusion of the simulation (50 years).

4. Results and Analysis

4.1 Overview

This chapter presents the results of the simulations described in Chapter 3. These results include breakthrough curves for Scenarios 1-3, mass storage comparisons, and the sensitivity analysis. The first moment analysis discussed in Chapter 3 was not used due to the absence of significant differences in the breakthrough curves.

4.2 Simulation Results

The figures and data presented in this section are for Scenarios 1-3. The MCL for TCE, 0.005 mg-L^{-1}, is shown in all plots for comparison.

4.2.1 Breakthrough Curves

Three breakthrough curves are shown below in Figure 4.1. These breakthrough curves plot concentration versus time for the total simulation time, 50 years (18250 days). Figure 4.1a is a plot of the concentrations at the observation point placed within the sand, Figure 4.1b is a plot of the concentrations observed at the observation point placed at the sand/clay interface, and Figure 4.1c is a plot of the concentrations observed at the observation point placed within the clay layer. All wells are 50m down gradient from the source zone.

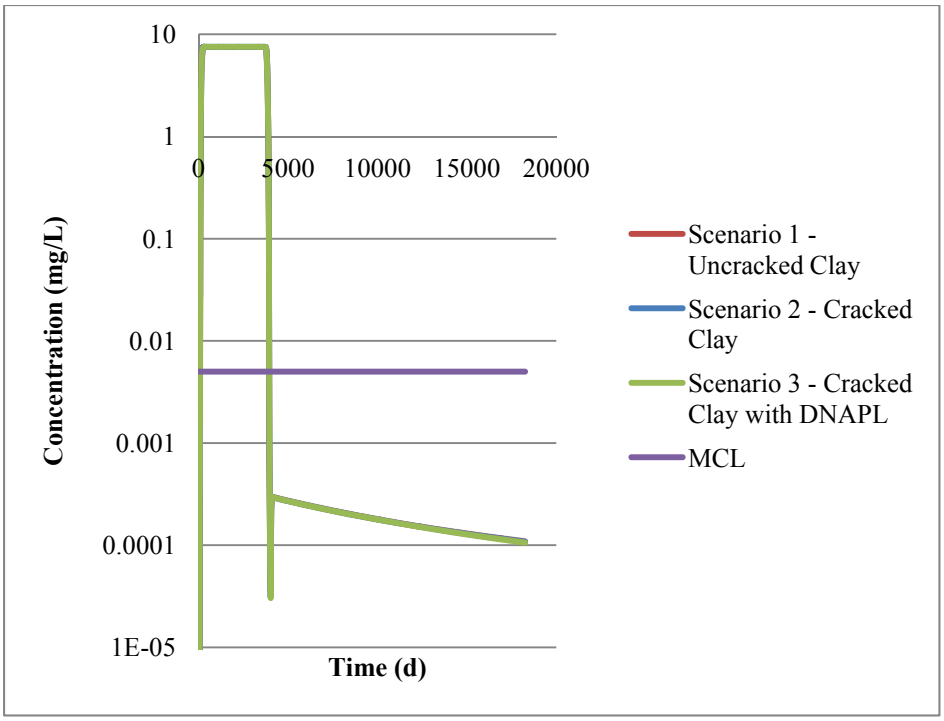
10
1
0.1
0.01
0.001
0.0001
1E-05
0
5000
10000
15000
20000
Concentration (mg/L)
Time (d)
Scenario 1 - Uncracked Clay
Scenario 2 - Cracked Clay
Scenario 3 - Cracked Clay with DNAPL
MCL

(a)

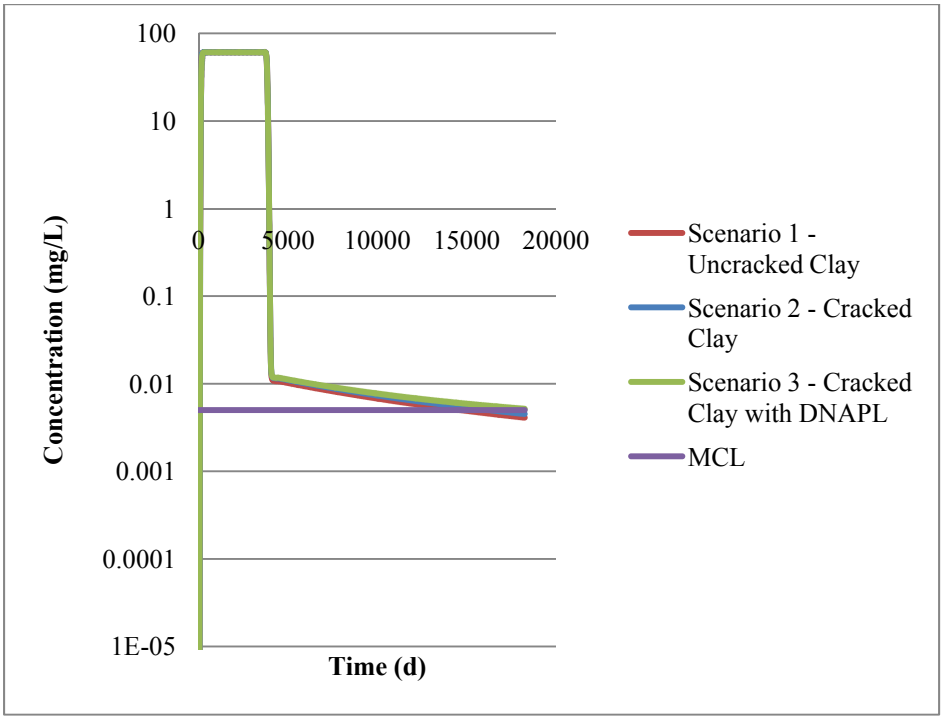
100
10
1
0.1
0.01
0.001
0.0001
1E-05
0
5000
10000
15000
20000
Concentration (mg/L)
Time (d)
Scenario 1 - Uncracked Clay
Scenario 2 - Cracked Clay
Scenario 3 - Cracked Clay with DNAPL
MCL

(b)

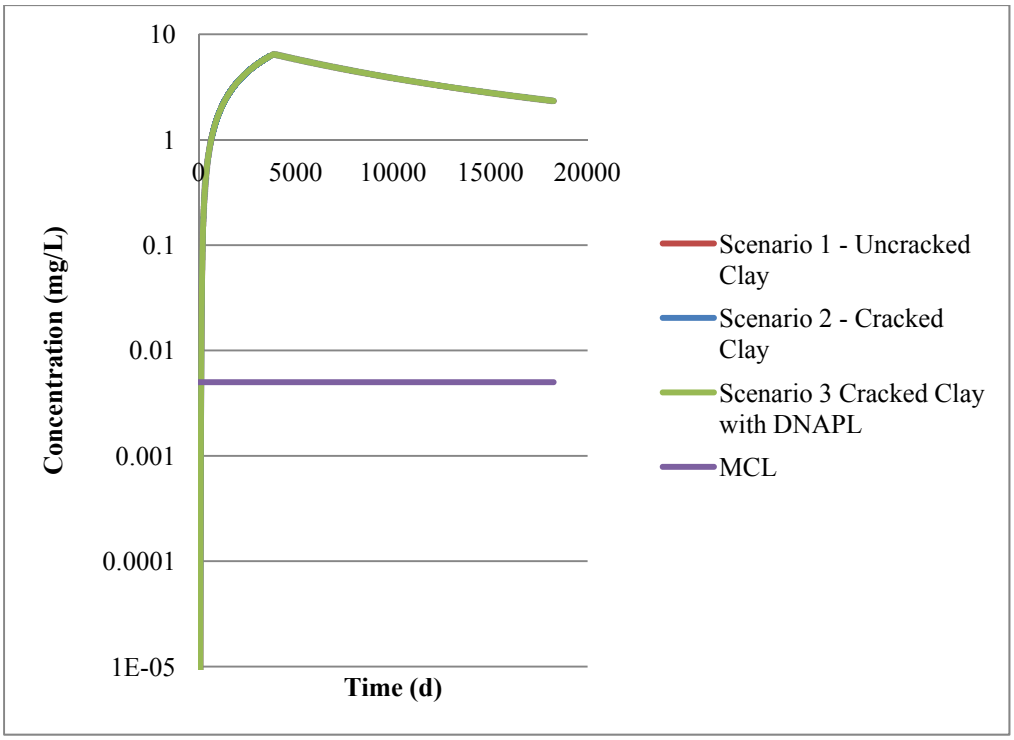

(c)

Figure 4-A: Breakthrough Curves (a) within sand layer, (b) at sand/clay interface, and (c) within clay layer

Qualitatively, the breakthrough curves for Scenarios 1-3 all display the expected behavior. At the observation points in high flow sand zones (4.1a and 4.1b), the concentration rises quickly when the source is present, and when the source is removed a rapid decrease is observed with back diffusion then causing the tailing. In the low flow clay zone, Figure 4.1c, the increase was much slower due to low flow rates in the low permeability layer and a relative increase in diffusive rather than advective transport into the low permeability layer.

Contrary to results presented in Miniter (2011), the concentration in the sand layer does not remain above the MCL for extended periods of time in Scenario 2. However,

consistent with the findings of Miniter (2011), at the sand clay interface and within the clay layer, the concentrations remain above the MCL for over forty years. Furthermore, the tailing seen at the sand-clay interface is similar to the tailing from back diffusion of TCE in a clayey silt aquitard observed by Chapman and Parker (2005). To further illustrate differences between the scenarios, curves are presented in Figure 4.2 over the time period beginning ten years after source removal (7300 days) and extending to fifty years.

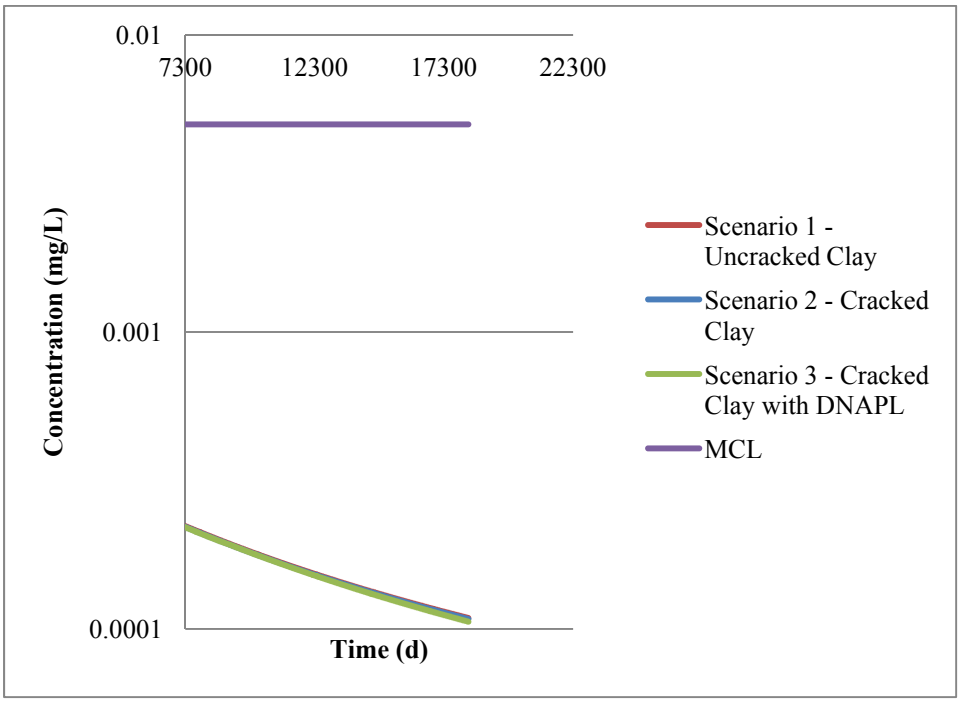

(a)

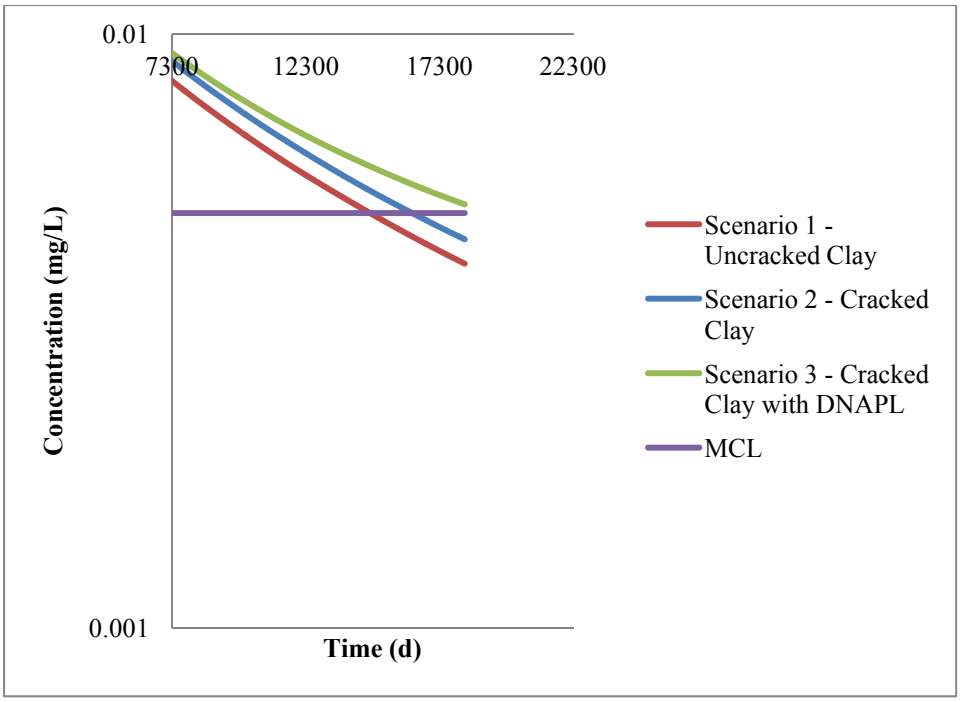

(b)

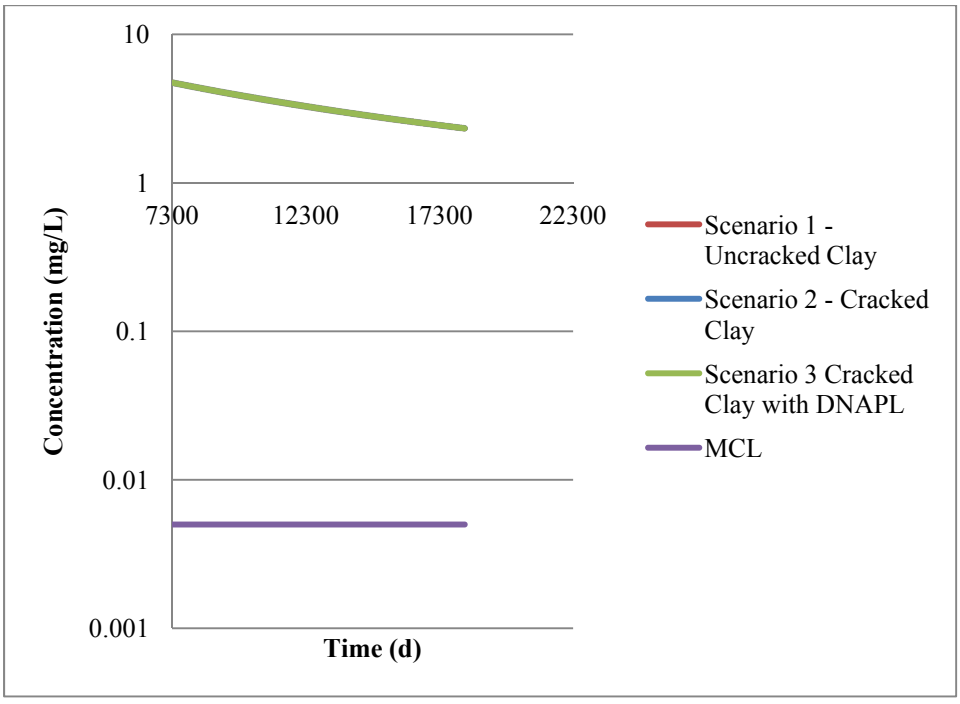

(c)

Figure 4-B: Breakthrough Curves (a) within sand layer, (b) at sand/clay interface, and (c) within clay layer

As Figure 4.2a shows, the concentrations of TCE within the sand layer and clay for all the scenarios appear to be the same for the entire duration of the simulation. These concentrations remain well below the MCL, indicating cracking may have little to no impact on down gradient concentrations 1 m above the low permeability layer. However, the concentrations observed at the sand-clay interface, shown in Figure 4.2b, do indicate a significant difference in down gradient concentrations associated with no cracking, cracking, and DNAPL storage and transport within cracks.

While the concentrations at the sand-clay interface remain within an order of magnitude of each other, the time at which the concentration decreases below the MCL is significantly different. In Scenario 1 the concentration drops below the MCL at 40.3 years, in Scenario 2 the corresponding time is 44.6 years, and in Scenario 3 the concentration remains above the MCL for the extent of the simulation. Further simulations concluded Scenario 3 dropped below the MCL at 52.6 years. Since the concentration breakthrough curves within the clay layer, shown in Figure 4.2c, are all the same, the differences observed at the sand/clay interface are most likely not due to back diffusion in the vicinity of the observation point, but rather due to up gradient contamination. This behavior can be explained by the liquid phase TCE stored within the cracks.

4.2.2 Mass Analysis

The goal of the mass analysis is to quantify the amount of TCE stored within the low permeability layer at different points in time; at the start of the simulation (0 years), immediately following source removal (10 years), and at the end of the simulation (50 years). The mass of stored TCE is the long term source for back diffusion, and therefore,

an important parameter to measure. The total mass is calculated for the entire 100 m x 70 m x 6 m clay layer, although the mass distribution is not determined. It is believed, though, that much of the mass is in the upper portion of the clay layer. It is important to note in order to simulate the effect of cracks in Scenario 3, the DNAPL saturation was set at the beginning of the simulation and again at the ten year point, as discussed in Chapter 3. Unfortunately this means between 0 and 10 years the DNAPL saturation is not held constant. Table 4.1 contains calculated TCE masses in the clay layer for Scenarios 1-3.

Table 4-1: Mass Analysis for Scenarios 1-3

	Scenario 1			Scenario 2			Scenario 3		
	0 yrs	10 yrs	50 yrs	0 yrs	10 yrs	50 yrs	0 yrs	10 yrs	50 yrs
Dissolved TCE (kg)	0	8.19	6.23	0	8.29	6.36	0	8.38	6.89
Sorbed TCE (kg)	0	0	0	0	0	0	0	0	0
DNAPL TCE (kg)	0	0	0	0	0	0	36.1	36.1	35.7
Total Mass TCE (kg)	0	8.19	6.23	0	8.29	6.36	36.1	44.4	42.6

As expected, the dissolved TCE mass at both 10 and 50 years increased from Scenarios 1 to 3. While the increase in mass is not significant, it may explain the tailing seen at the sand-clay interface in Figure 4.2b. In both Scenarios 1 and 2 the dissolved mass decreased by approximately 1.9 kg between years 10 and 50, while in Scenario 3 the decrease was only 1.5 kg. The higher aqueous concentrations observed in Scenario 3 are most likely due to the dissolution of the DNAPL. Further examination is required to determine if dissolution of TCE will sustain aqueous concentrations in the aquifer above the MCL.

4.4.3 Sensitivity Analysis

The goal of the sensitivity analysis was to determine which input values significantly impacted breakthrough tailing at the observation points and the total mass

storage in the low permeability layer. Scenario 3 was used as the baseline scenario for this analysis in order to capture all important processes. The values changed include the first order DNAPL dissolution rate constant (β), and the vertical hydraulic conductivity (K_v) of the cracked clay directly below the source. Table 4.2 indicates both the baseline and sensitivity analysis values.

Table 4-2: Sensitivity Analysis Values

	Lower Sensitivity Analysis Vaslue	Baseline Value	Upper Sensitivity Analysis Value
β (d^{-1})	4.45E-5	0.00445	0.445
K_v (m-d^{-1})	4.32E-6	0.000432	0.0432

With the changes in β and K_v no discernible differences were observed in the clay and sand breakthrough curves; however, noticeable changes occurred at the sand-clay interface. The breakthrough curve at the sand-clay interface for varying β and K_v is presented below in Figure 4.3(a) and (b). The plot includes the curves generated using the baseline values as well as using the sensitivity analysis values. A mass analysis was used in conjunction with breakthrough curves to quantify the effect of varying β and K_v. The results of the mass analysis are shown below in Table 4.3. The results of Scenario 3 with baseline values are also shown in Table 4.3 for comparison.

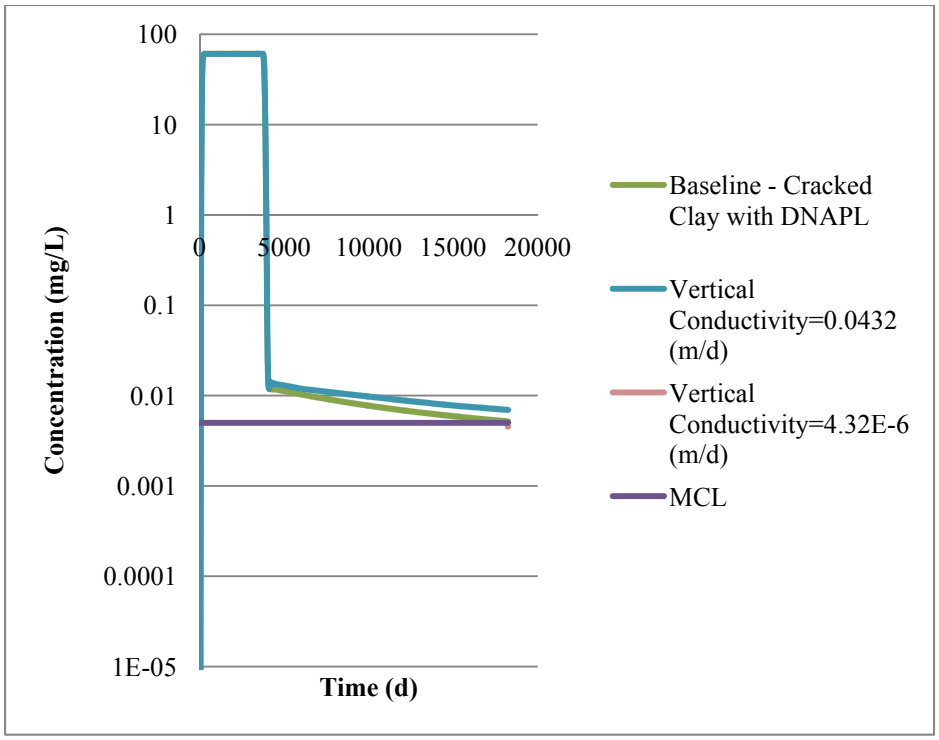

(a)

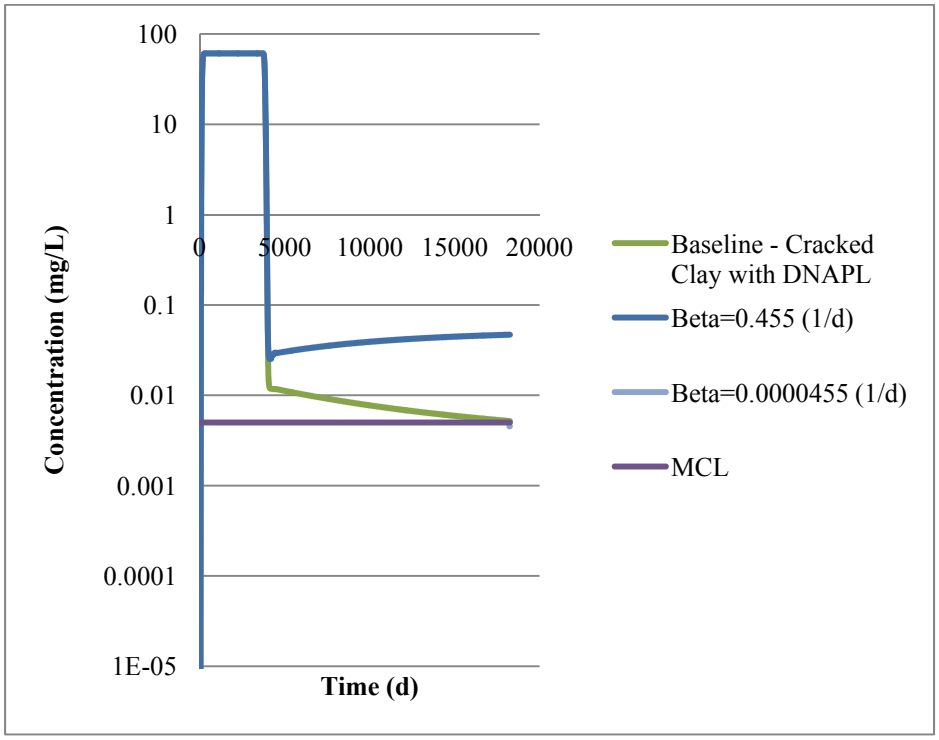

(b)

Figure 4-C: Breakthrough Curve at Sand-Clay Interface for Sensitivity Analysis: (a) β and (b) K_v

Table 4-3: Mass Analysis for Sensitivity Analysis

	Scenario 3 - β=0.0000455 d^{-1}			Scenario 3			Scenario 3 - β=0.455 d^{-1}		
	0 yrs	10 yrs	50 yrs	0 yrs	10 yrs	50 yrs	0 yrs	10 yrs	50 yrs
Dissolved TCE (kg)	0	8.3	6.5	0	8.38	6.89	0	15.6	29.4
Sorbed TCE (kg)	0	0	0	0	0	0	0	0	0
DNAPL TCE (kg)	36.1	36.1	36.1	36.1	36.1	35.7	36.1	28.7	0.1
Total Mass TCE (kg)	36.1	44.3	42.6	36.1	44.4	42.6	36.1	44.3	29.5

	Scenario 3 - K_v=4.32E-6 m-d^{-1}			Scenario 3			Scenario 3 - K_v=0.0432 m-d^{-1}		
	0 yrs	10 yrs	50 yrs	0 yrs	10 yrs	50 yrs	0 yrs	10 yrs	50 yrs
Dissolved TCE (kg)	0	8.22	6.73	0	8.38	6.89	0	8.61	7.13
Sorbed TCE (kg)	0	0	0	0	0	0	0	0	0
DNAPL TCE (kg)	36.1	36.1	35.8	36.1	36.1	35.7	36.1	36.1	35.8
Total Mass TCE (kg)	36.1	44.3	42.5	36.1	44.4	42.6	36.1	44.7	42.9

When β was increased, a large increase in tailing was noticed. As β is the parameter that represents the effects of dissolution, the increase in tailing can be attributed to the dissolution of the DNAPL. Since the rate of dissolution is larger, the rate of mass transport of CAH into the aqueous phase and into the high permeability layer is larger. Note that due to model limitations, the extent of tailing may be even more pronounced in a real scenario, as the model used in this study does not allow for replenishment of the DNAPL in the cracks by the DNAPL pool sitting atop the clay layer. As Figure 4.3a shows, it appears that the concentration is still increasing at the end of the simulation. This trend is also observed in the mass analysis, which shows the aqueous concentration at the source increasing significantly after the source is removed, due to faster DNAPL dissolution at the source. This indicates DNAPL within the cracks at the source can contribute significantly to down gradient plume concentrations for an extended period of time. When β was decreased, no change was detected from the

baseline scenario. This indicates the value used in Scenario 3 may be artificially low. We should note that the β values employed in these simulations were based on pure TCE, not TCE waste found at contaminated sites. A quantification of β for TCE waste is needed to realistically simulate the behavior of DNAPL waste at sites where the DNAPL waste has penetrated cracks.

In this research, cracks are approximated by an equivalent hydraulic conductivity; as cracking increases so does the vertical hydraulic conductivity (K_v). The vertical conductivity was increased to account for cracks based on the general observation that cracking increases the overall vertical hydraulic conductivity by two to three orders of magnitude. A correlation between vertical hydraulic conductivity and crack characteristics such as crack aperture, spacing, and depth would be useful in determining reasonable estimates for vertical hydraulic conductivity in future simulations. In this sensitivity analysis, when the vertical conductivity increased, tailing also increased. After the initial ten years, the mass within the clay layer in the Scenario 3 with the increased vertical hydraulic conductivity is similar to that in the baseline Scenario 3; however, 40 years after source removal, the mass in the former scenario is higher than that in the latter. The results of this sensitivity analysis indicate more cracking can lead to higher down gradient concentrations for extended periods of time.

5 Conclusions and Recommendations

5.1 Conclusions

This research modeled the effect of cracking in low permeability layers on the storage and transport of TCE. The effect of cracking on transport was measured by comparing breakthrough curves at down gradient monitoring points as well as by calculating the quantity of TCE stored in the low permeability clay layer.

The model simulated cracks through an increase in the vertical conductivity at the source. This change was hypothesized to simulate enhanced diffusion of TCE into the low permeability layer. In the model the source was present for ten years allowing for contaminant transport into and storage within the low permeability layer. The source was then removed and down gradient concentrations were simulated at three observation points for an additional forty years to determine the impact of cracking. Three scenarios were studied, (1) transport into uncracked clay, (2) transport of the dissolved TCE into cracked clay, and (3) transport of DNAPL phase TCE into cracked clay. Down gradient concentrations were sustained by back diffusion of TCE from the low permeability layer. Based on the results of the mass analysis and breakthrough curves it was determined that:

(1) Cracking (as approximated with an increase in vertical conductivity and a DNAPL saturation) will cause an increase in TCE transport into the low permeability layer
(2) Enhanced transport of TCE into the source zone will sustain down gradient concentrations above the MCL at the sand-clay interface

(3) Down gradient concentrations are sustained due to back diffusion from the source zone

(4) DNAPL phase TCE within cracks can significantly contribute to down gradient concentrations; however, this contribution is dependent upon the rate of DNAPL dissolution

(5) Remediation goals may be impossible to meet within a prescribed time frame if source remediation strategies are used which do not account for the increased back diffusion out of cracked low permeability layers at contaminated sites.

5.2 Recommendations for Future Research

The limitations of the model used in this research inherently provide future opportunities for research. This work approximates cracking in the source zone through an increase of the vertical hydraulic conductivity. While this assumption may permit enhanced transport, the use of an adaptable grid model would allow for the direct modeling of cracks. If an adaptable grid model is used, it might be possible to model pressure dependent NAPL transport into the cracks for the duration of source exposure. Further, direct crack modeling would only simulate increased flow through cracks as opposed to the whole matrix, meaning diffusion out of the uncracked clay may in fact be a much slower process. The results of Ayral et al. (2011) indicate that TCE DNAPL waste can cause cracking in clay; this means if DNAPL is stored within existing cracks, the crack properties may change allowing for further diffusion into the matrix.

In order to evaluate the ability of this model to predict field scale conditions, the model should be applied to a well characterized site that is known to display back diffusion after

source zone remediation. While cracking may be unknown at the site, a variety of hydraulic conductivities can be tested to determine if cracking can be an explanation of long term plume persistence above target MCLs.

This research used dissolution and diffusion values for pure TCE. TCE waste can have very different properties due to the presence of other chemicals; therefore further research could determine and incorporate realistic chemical properties of TCE waste into simulations. This model also does not account for chemical or biological contaminant degradation. TCE degradation could significantly impact the down gradient concentration; however, if degradation is modeled it would be important to also model TCE daughter product formation.

Appendix A

Open GMS

Start Up

Save your file – Be sure to save after every few steps as GMS can crash frequently.

The units are not assumed to be SI units. The units used in the Sievers thesis are SI units.

Edit => Units…

The required packages for running simulations are MODFLOW and MT3D, RT3D, SEAM3D.

Edit => Model Interfaces => Check MODFLOW and MT3D, RT3D, SEAM3D boxes

Create Grid

On Bottom of screen click 3D Grid symbol (Green 3D cube) shown in Figure A.1

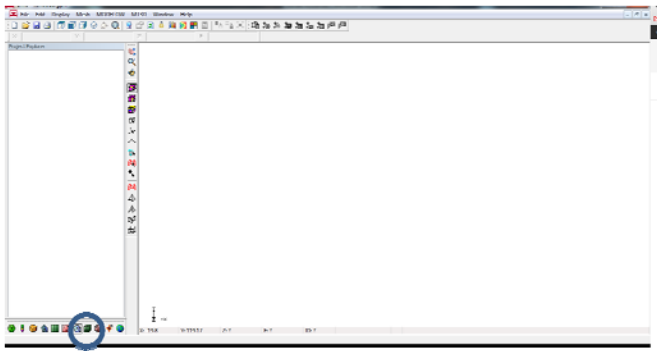

Figure A. 1: 3D grid symbol

Once the 3D Grid is selected a Grid dropdown menu will appear in the upper toolbar next to Display

Grid => Create Grid

Input dimensions of grid. Make origin at (0,0,0). Sievers grid is x = 100m y=70m z=12m. Be sure to put number of cells the same as dimensions to ensure $1m^3$ grid blocks.

Input Matrix Characteristics

Edit => Materials – See table 3.1 for relevant characteristics

Create MODFLOW Simulation

MODFLOW => New Simulation

The MODFLOW Global/Basic Package will pop up

- MODFLOW Version – Use MODFLOW 2000 version (2005 version not compatible with Huang model)
- Run Options – Select Forward Run
- Model Type – Select Steady State
- Packages => Flow Package – Select Layer Property Flow (LPF)
- Packages => Solver – Pre-Cond. Conj. Grad (PCG2)
- IBOUND => In all layers set farthest left and right column to -1, all other cells to 1 shown in Figure A.2

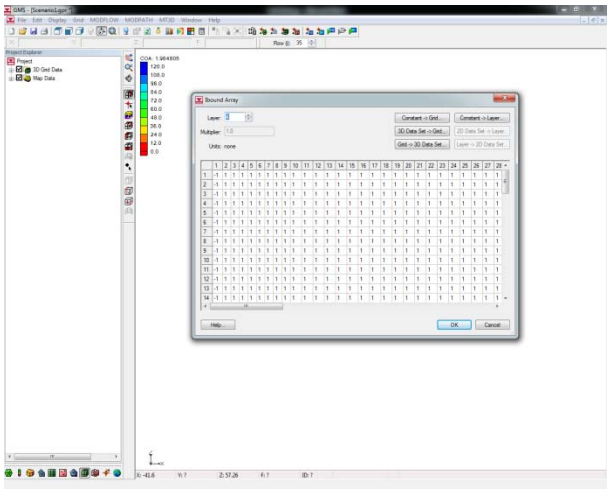

Figure A. 2: IBOUND input

- Starting Heads => The only cells which will remain constant are the ones with a -1 value in the IBOUND array. Sievers thesis set 1 m head difference, farthest left column to 20.5 farthest right to 19.5m shown in Figure A.3.

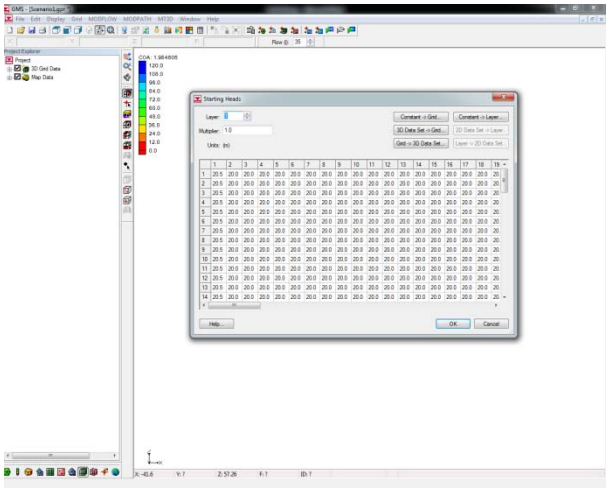

Figure A. 3: Initial head conditions

- Top Elevation/Bottom Elevation => Sanity check, should be 1m difference between each layer, as well as a 1m difference for top and bottom for same layer

MODFLOW => LPF Package

- Layer Property Entry Method – Select use material IDs (seems to be easiest way)
- Layer type – Ensure for Layer 1 confined is selected
- Vertical hydraulic conductivity – Specify K_v for all layers
- Material IDs => For grid input numbers corresponding to material type (Layers 1-6 are sand, Layers 7-12 are a combination of cracked and uncracked clay)
- Interblock transmissivity – Harmonic mean
- Cell wetting parameters – Do not select Allow wetting of cells

MODFLOW => Run MODFLOW

Create Observation Wells

Right click on Project in Project Explorer Window => New => Conceptual Model shown in Figure A.4

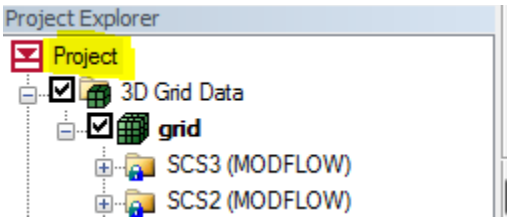

Figure A. 4: Image of project explorer

Conceptual Model Properties box will pop up – Select Transport – Select RT3D – Select User Defined Reaction – Define aqueous species name – Click OK

Map Data will now be in Project Explorer Window – Right click New Model – select New Coverage

Coverage Setup will pop up – Select defined species under Observation Points – Click OK shown in Figure A.5

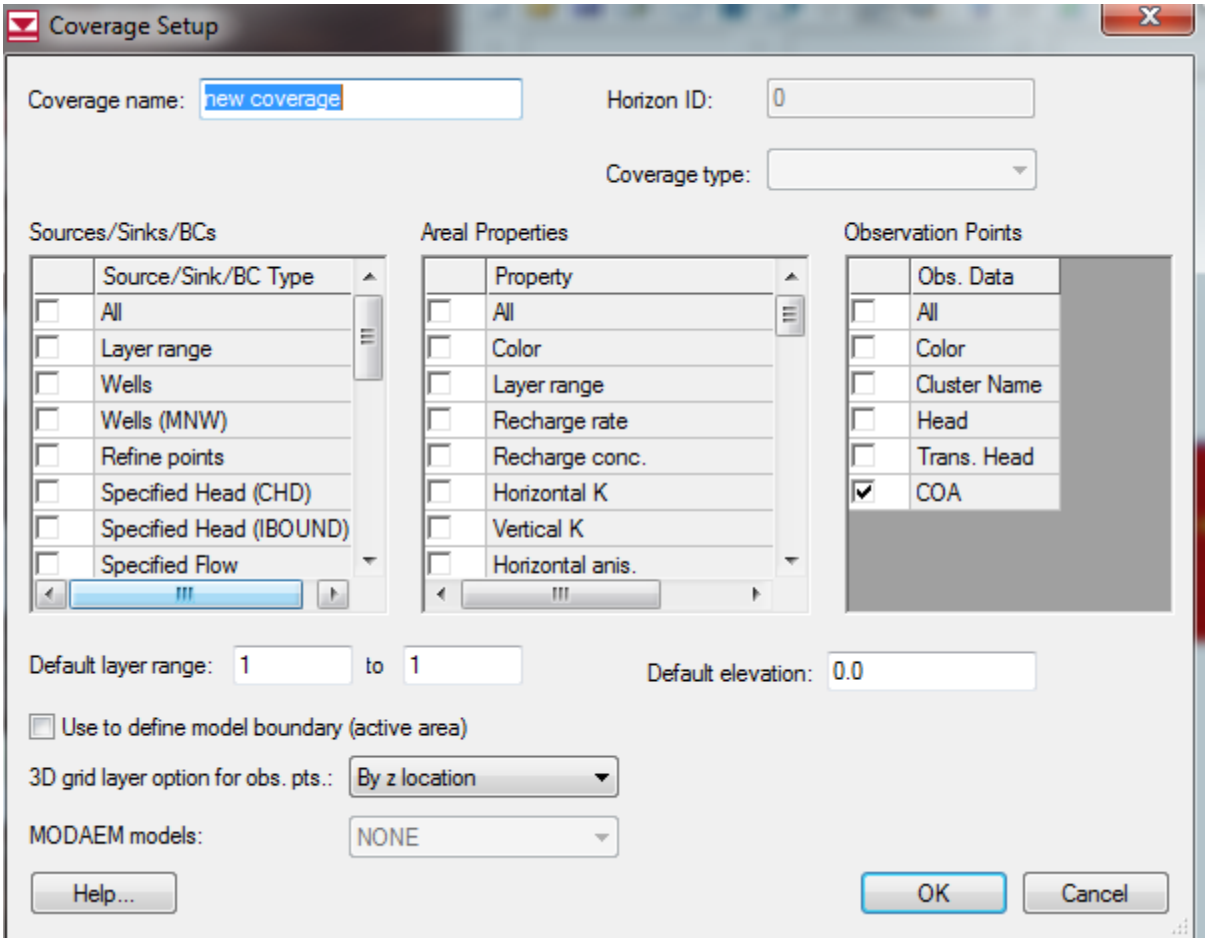

Figure A. 5: Coverage set up

Right click New Coverage – Attribute Table – Enter coordinates for observation wells – select obs. pt for Type shown in Figure A.6

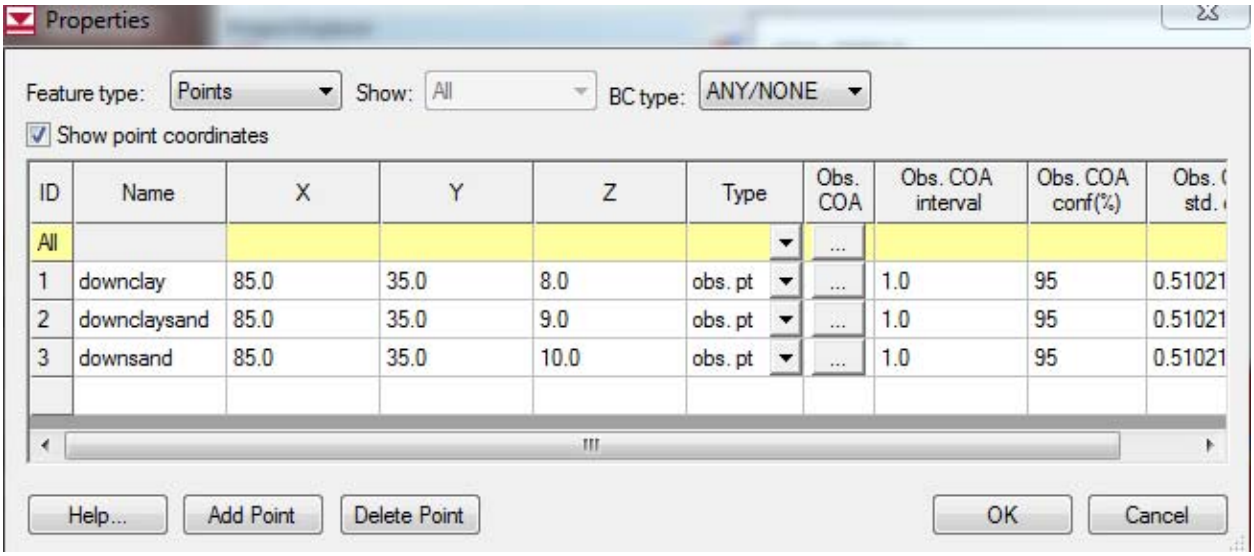

Figure A. 6: Observation point properties

Create RT3D Simulation

MT3D => New Simulation

The MT3D Basic Transport Package will pop up shown in Figure A.7

- Model – Select RT3D
- Stress Periods – Can be changed by user for different simulations
- Output Control – Ensure print or save at specified interval is chosen for breakthrough curve data, always select Save binary concentration file and Save mass balance file
- Packages – Select Advection Package, Dispersion Package, Source/sink mixing package, Chemical reaction package (select User-defined Reaction), GCG solver package
- Define Species – Define three species, COA, NAPLsoil, NAPLsaturation. Order does matter. COA is the only mobile species.

- Layer Data – Select use materials for porosity and long. Dispersivity and HTOP equals top of layer 1
- Starting Concentration – Can be defined for all species based on goal of simulation

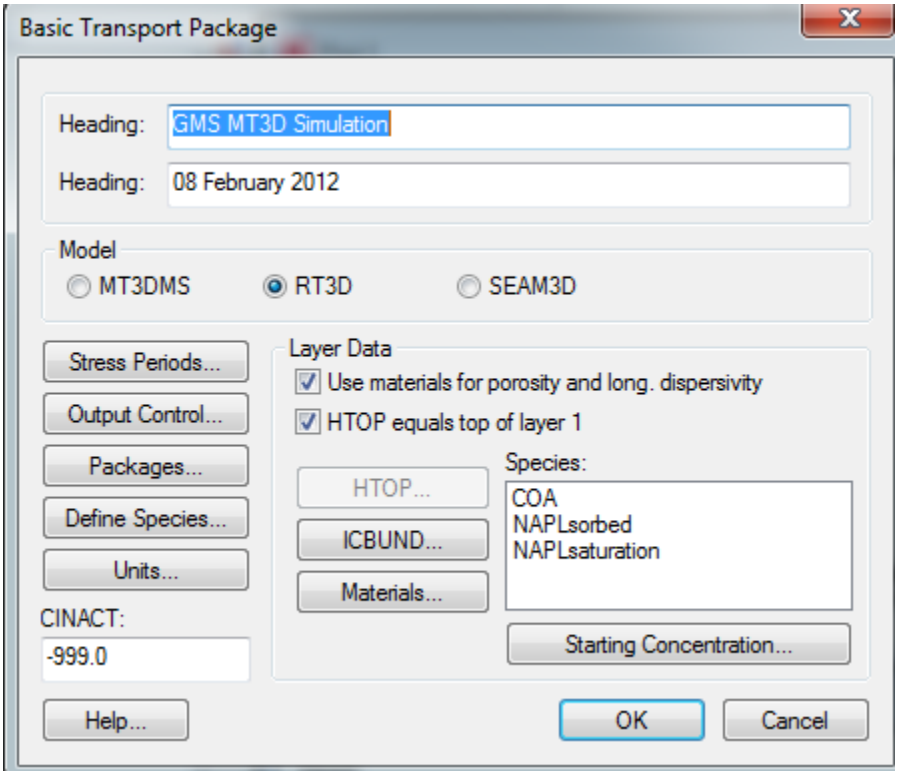

Figure A. 7: RT3D Basic Transport Package window

MT3D => Advection Package – Select Third order TVD scheme (ULTIMATE)

MT3D => Dispersion Package – Input appropriate parameters

MT3D => Source/Sink Mixing Package – This is where the simulated source is input – need one data point for each grid block (192 for 192m^3 source zone) shown below in Figure A.8.

- Layer – Should be the layer immediately above the low permeability layer

- Type – specconc
- COA – This column will be whatever you define as your mobile species

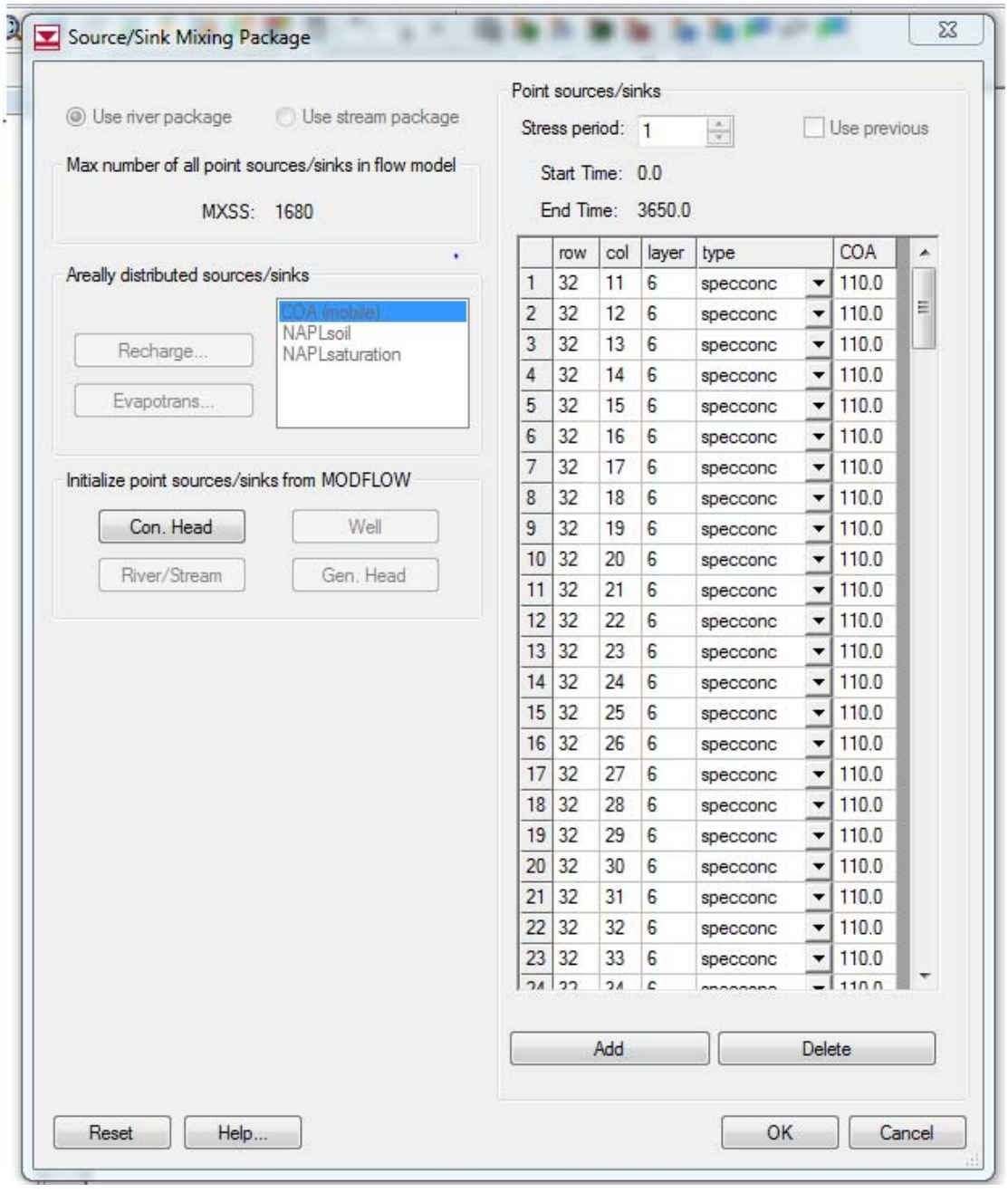

Figure A. 8: Source/Sink Mixing Package initial conditions

MT3D => Chemical Reaction Package => Define Parameters (Order matters, also, cannot be spatially varied) shown in Figure A.9

- Modop – Always select 6
- Rho_bulk – Bulk density of media (mg/L) – Note, only one bulk density can be set since it cannot be spatially varied, so for entire array use clay bulk density.
- Rho_NAPL – Bulk density of NAPL (mg/L)
- Alpha – First order mass transfer constant (d^{-1})
- Kd – Sorption coefficient (mg/L)
- Beta – First order dissolution constant (d^{-1})
- Cs – NAPL solubility (mg/L)

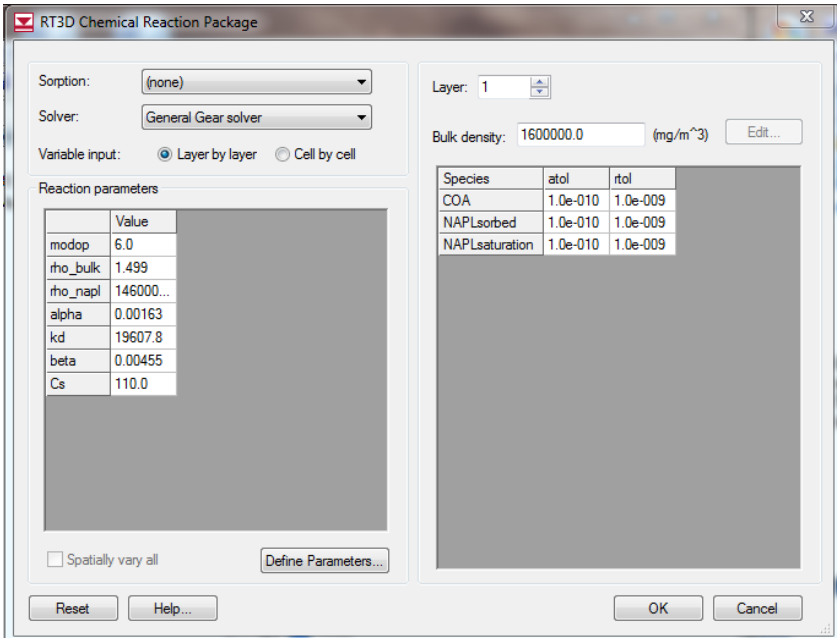

Figure A. 9: Chemical Reaction Package

MT3D => Run RT3D

Read Results

Breakthrough Curve Data

Display => Plot Wizard – Select Time Series – Next – Select Show All – Finish

Once chart appears, right click on axis and select Export/Print – Select Text/Data – Select File (Pick destination by clicking on Browse) – Select Export – Select Maximum Precision – Select Export

Breakthrough curve data can be generated in Excel from Exported data file.

Mass Data

After simulation is complete Save. It is important data is gathered from the desired time. To ensure desired time is selected, select species in home screen, then time under Project Explorer shown in Figure A.10.

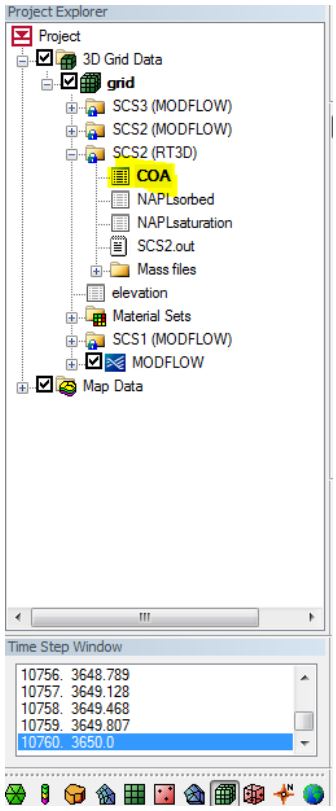

Figure A. 10: Select data set for mass analysis

MT3D => Basic Transport Package => Select Species => Starting Concentration => 3D Data Set -> Grid shown in Figure A.11

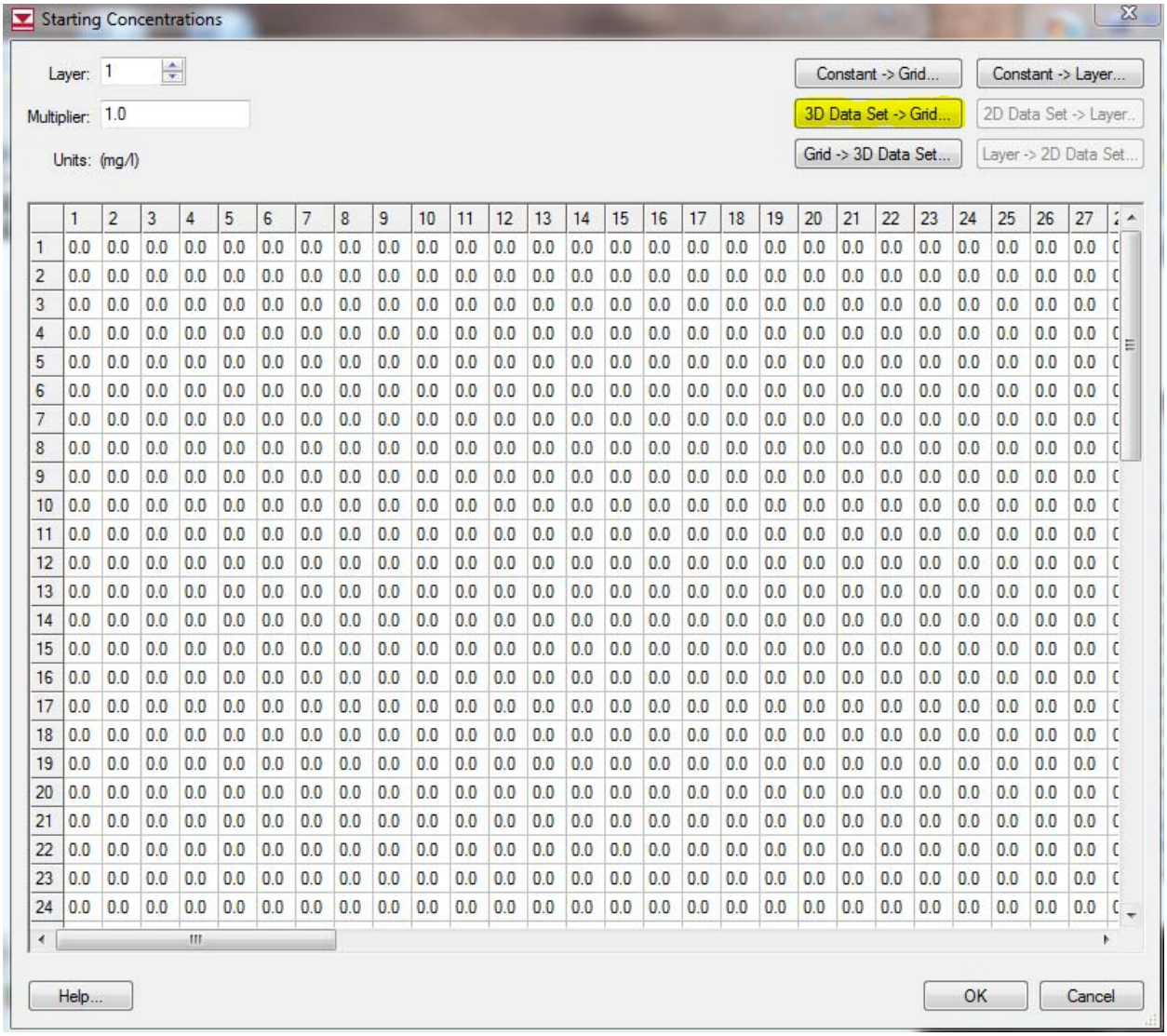

Figure A. 11: Import 3D data set

Once clicked, box shown below will appear. Select your RT3D data set, then the species you want to study. It is important to ensure the time selected is the end time in the simulation shown in Figure A.12.

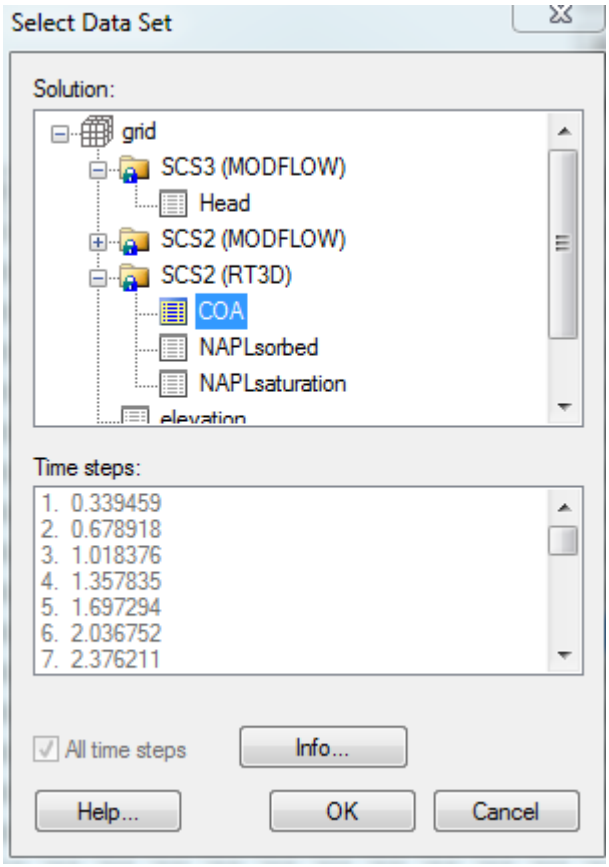

Figure A. 12: Select data set for import

Grid will then be filled with data. Copy pertinent data into Excel. Click Cancel after data has been removed.

Simulation with No Source Present

The following instructions are for after the source has been removed. Save file as a different name, rerun MODFLOW. Delete all entries in Source/Sink Mixing Package. Follow directions above for Mass Data, however do not click cancel once data sets are imported into grid, click OK. Change Stress Period to desired length, then run RT3D.

Bibliography

AFCEE, Air Force Center for Engineering and the Environment. *AFCEE Source Zone Initiative Final Report*. Brooks AF Base: US Air Force, 2007.

Aryal, D., M. Otera, A. Demond, M. Goltz, and J. Huang. Impact of Chlorinated Waste Solvents on the Structure of Clay in Low Permeability Zones in Groundwater Contamination Source Areas. *SERDP*., 2011.

Ayral, D., M. Otera, A. Demond, M. Goltz, and J. Huang. Impact of Chlorinated Waste Solvents on the Structure of Clay in Low Permeability Zones in Groundwater Contamination Source Areas. *SERDP*., 2011.

Ball, W. P., L. Chongxuan, X. Gunoshou, and D. F. Young. A diffusion-based interpretation of tetrachloroethene and trichloroethene concentration profiles in a groundwater aquitard. *Water Resources Reasearch*. 33(12): 2741-2757, 1997.

Brown, K. W. and C. J. Thomas. A Mechanism by with Organic Liquids Increase the Hydraulic Conductivity of Compacted Clay Materials. *Soil Science Society of America Journal*. 51(6): 1451-1459, 1987.

Chapman, S. M. and B. Parker. High Resolution Field Characterization and Numerical Modeling for Analysis of Contaminant Storage and Release from Lower Permeability Zones. *SERDP*., 2011.

Christ, J.A., C. A. Ramsburg, K. D. Pennell, and L. M. Abriola. Estimating mass discharge from dense nonaqueous phase liquid source zones using upscaled mass transfer coefficients: An evaluation using multiphase numerical simulations. *Water Resources Research*. 42: 1-13, 2006.

Cihan, A. and J. S. Tyner. 2-D radial analytical solutions for solute transport ina dual-porosity medium. *Water Resources Research*. 47: 1-11, 2011.

Clark, M. *Transport modeling for environmental engineers and scientists*. John Wiley and Sons, 2009.

Culver, T. B., S. P. Hallisey, D Sahoo, J. J. Deitsch, and J. A. Smith. Modeling the Sesorption of Organic Contaminants from Long-Term Contaminated Soil Using Distributed Mass Transfer Rates. *Environmental Science and Technology*. 31(6): 1581-1588, 1997.

Demond, A. Impact of Chlorinated Solvents on the Structure of Clay in Low Permeability Zones in Groundwater Contamination Source Areas. *In*: *SERDP*. Washington DC, 2010.

Denness, P. and B. Fookes. Observational Studies on Fissure Patterns in Crestaceous Sediments of South-East England. *Geotechnique*. 19(4): 453-477, 1969.

EPA. *Basic Information about Regulated Drinking Water Contaminants*. [online]. [Accessed 15 May 2011]. Available from World Wide Web: <http://water.epa.gov/drink/contaminants/basicinformation/trichloroethylene.cfm>

Esposito, S.J. and N. R. Thomson. Two-phase flow and transport in a single fracture-porous medium system. *Journal of Contaminant Hydrology*. 37: 319-341, 1999.

Grisak, G.E. and J.F. Pickens. Solute transport through fractured media 1. the effect of matrix diffusion. *Water Resources Research*. 16(4): 719-730, 1980.

Gupta, R. S. *Hydrology and Hydraulic Systems*. Long Grove: Waveland Press Inc., 2008.

Hinsby, K., L. D. McKay, P. Jorgensen, M. Lenczewski, and C. P. Gerba. Fracture Aperture Measurements and Migration of Solutes, Viruses, and Immiscible Creosote in a Column of Clay-Rich Till. *Ground Water*. 34(6): 1065-1075, 1996.

Johnson, R., J. Cherry, and J. Pankow. Diffusive contaminant transport in natural clay: a field example and implications for clay-lined waste disposal sites. *Environ. Sci. Technol.* 23(3): 340-349, 1989.

Kueper, B.H. and D.B. McWhorter. The behavior of dense, nonaqueous phase liquids in fractured clay and rock. *Ground Water*. 29(5): 716-728, 1991.

Mackay, G.M., R.D. Wilson, M.J. Brown, W.P. Ball, D.P. Durfee, G.Xia, and C. Liu. A controlled field evaluation of continuous versus pulsed pump-and-treat remediation of a VOC-contaminated aquifer: Site characterization, experimental setup, and overview of results. *Journal of Contaminant Hydrology*. 41(1): 81-131, 2000.

McKay, L. D., J. A. Cherry, and Gillham R. W. Field Experiments in a Fractured Clay Till 1. Hydraulic Conductivity and Fracture Aperture. *Water Resources Research*. 29(4): 1149-1162, 1993.

McKay, L. D. and J. Fredericia. Distribution, origin, and hydraulic influence of fractures in a clay-rich glacial deposit. *Canadian Geotechnical Journal*. 32: 957-975, 1995.

Miniter, Jeremy. Modeling Enhanced Storage of Groundwater Contaminants Due to the Presence of Cracks in Low Permeability Zones Underlying Contaminant Source Areas. Wright Patterson AFB, March 2011.

Miniter, J. *Modeling Enhanced Storage of Groundwater Contaminants Due to the Presence of Cracks in Low Permeability Zones Underlying Contaminant Source Areas*. Dayton, 2011.

Murphy, J.R. and N.R. Thomson. Two-phase flow in a variable aperture fracture. *Water Resources Research*. 29(10): 3453-3476, 1993.

O'Hara, S. K., B. L. Parker, P. R. Jorgensen, and J. A. Cherry. Trichlorothene DNAPL flow and mass distribution in naturally fractured clay: Evidence of aperture variability. *Water Resources Research*. 36(1): 135-147, 2000.

Parker, B. L., S. W. Chapman, and M. A. Guilbeault. Plume Persistance Caused by Back Diffusion from Thin Clay Layers in a Sand Aquifer Following TCE Source-Zone Hydraulic Isolation. *Journal of Contaminant Hydrology*. 102(1-2): 86-104, 2008.

Parker, B.L, S.W. Chapman, and M.A. Guilbeault. Plume persistence caused by back diffusion from thin clay layers in a sand aquifer following TCE source-zone hydraulic isolation. *Journal of Contaminant Hydrology*. 102: 86-104, 2008.

Parker, B. L., J. A. Cherry, and S. W. Chapman. Field study of TCE diffusion profiles below DNAPL to assess aquitard integrity. *Journal of Contaminant Hydrology*. 74(1-4): 197-230, 2004.

Parker, B. L., R. W. Gilham, and J. A. Cherry. Diffusive Dissaperance of Immiscible-Phase Organic Liquids in Fractured Geologic Media. *Ground Water*. 32(5): 805-820, 1994.

Reynolds, D.A. and B.H. Kueper. Numerical examination of the factors controlling DNAPL migration through a single fracture. *Ground Water*. 40(4): 368-377, 2002.

Rowe, R. K. and J. R. Booker. Contaminant migration through fractured till into an underlying aquifer. *Canadian Geotechnical Journal*. 27: 484-495, 1990.

Sale, T.C., J.A. Zimbron, and D.S. Dandy. Effects of reduced contaminant loading on downgradient water quality in an idealized two-layer granular porous media. *Journal of Contaminant Hydrology*. 102: 72-85, 2008.

Sale, T. C., J. A. Zimbron, and D. S. Dandy. Effects of reduced contaminant loading on downgradient water quality in an idealized two-layer granular porous media. *Journal of Contaminant Hydrology*. 102: 72-85, 2008.

Sims, J. E, D. Elsworth, and J. A. Cherry. Stress-dependant flow through fractured clay till: a laboratory study. *Geotechnique*. 33: 449-457, 1996.

REPORT DOCUMENTATION PAGE

Form Approved
OMB No. 074-0188

1. REPORT DATE *(DD-MM-YYYY)*	**2. REPORT TYPE**	**3. DATES COVERED** *(From – To)*
22-03-2012	Masters Thesis	Sep 2010 – Mar 2012

4. TITLE AND SUBTITLE
Modeling the Impact of Cracking in Low Permeability Layers in a Groundwater Contamination Source Zone on Dissolved Contaminant Fate and Transport

5a. CONTRACT NUMBER

5b. GRANT NUMBER

5c. PROGRAM ELEMENT NUMBER

6. AUTHOR(S)
Sievers, Katherine W., 2nd Lieutenant, USAF

5d. PROJECT NUMBER
JON 11V193

5e. TASK NUMBER

5f. WORK UNIT NUMBER

7. PERFORMING ORGANIZATION NAMES(S) AND ADDRESS(S)

Air Force Institute of Technology
Graduate School of Engineering and Management (AFIT/EN)
2950 Hobson Way, Building 640
WPAFB OH 45433-7765

8. PERFORMING ORGANIZATION REPORT NUMBER

AFIT/GES/ENV/12-M02

9. SPONSORING/MONITORING AGENCY NAME(S) AND ADDRESS(ES)
Dr. Andrea Leeson
Strategic Environmental Research and Development Program
901 N. Stuart St., Ste 303
Arlington, VA 22203
Phone: 703-696-2118
E-Mail: Andrea.Leeson@osd.mil

10. SPONSOR/MONITOR'S ACRONYM(S)
SERDP

11. SPONSOR/MONITOR'S REPORT NUMBER(S)

12. DISTRIBUTION/AVAILABILITY STATEMENT
APPROVED FOR PUBLIC RELEASE; DISTRIBUTION UNLIMITED

13. SUPPLEMENTARY NOTES
This material is declared a work of the U.S. Government and is not subject to copyright protection in the United States

14. ABSTRACT
The storage and transport of a dense non-aqueous phase liquid (DNAPL) was evaluated using a numerical model. Many DNAPLs are used as solvents by the DoD and industry. The improper disposal and handling of these chemicals has led to long term contamination of groundwater. When spilled, a DNAPL will pool atop low permeability layers and slowly dissolve creating a contaminant plume. The dissolved contaminant within a low permeability layer serves as long-term sources of contamination once the source is removed. In this study, cracks are hypothesized to exist in the low permeability layers, allowing for enhanced transport. A numerical model is employed using a dual domain construct (high and low permeability layers) to investigate the impact of cracking on DNAPL and CAH movement. Three scenarios were modeled to evaluate the impact of cracks: (1) CAH diffusion into an uncracked low permeability clay layer; (2) CAH advection-dispersion into cracks, and (3) separate phase DNAPL movement into the cracks. This study found cracking will cause an increase in transport and storage of TCE into low permeability layers, and that this increased transport will sustain down gradient concentrations for decades. Further, DNAPL phase TCE within cracks can significantly contribute to down gradient concentrations.

15. SUBJECT TERMS
DNAPL, cracking, clay, back diffusion, enhanced diffusion, Groundwater Modeling System (GMS), dissolved phase plume, dual domain model

16. SECURITY CLASSIFICATION OF:			**17. LIMITATION OF ABSTRACT**	**18. NUMBER OF PAGES**	**19a. NAME OF RESPONSIBLE PERSON**
a. REPORT	**b. ABSTRACT**	**c. THIS PAGE**			MARK N. GOLTZ, ENV
U	U	U	UU	99	**19b. TELEPHONE NUMBER** *(Include area code)* (937) 255-3636

Standard Form 298 (Rev. 8-98)
Prescribed by ANSI Std. Z39-18

Form Approved
OMB No. 074-0188